



**HAL**  
open science

## Metal and metal oxide nanoparticles in the voltammetric detection of heavy metals: A review

Simona Sawan, Rita Maalouf, Abdelhamid Errachid, Nicole Jaffrezic-Renault

### ► To cite this version:

Simona Sawan, Rita Maalouf, Abdelhamid Errachid, Nicole Jaffrezic-Renault. Metal and metal oxide nanoparticles in the voltammetric detection of heavy metals: A review. Trends in Analytical Chemistry, 2020, 131, pp.article number 116014. 10.1016/j.trac.2020.116014 . hal-03023839

**HAL Id: hal-03023839**

**<https://hal.science/hal-03023839>**

Submitted on 25 Nov 2020

**HAL** is a multi-disciplinary open access archive for the deposit and dissemination of scientific research documents, whether they are published or not. The documents may come from teaching and research institutions in France or abroad, or from public or private research centers.

L'archive ouverte pluridisciplinaire **HAL**, est destinée au dépôt et à la diffusion de documents scientifiques de niveau recherche, publiés ou non, émanant des établissements d'enseignement et de recherche français ou étrangers, des laboratoires publics ou privés.

# Metal and Metal Oxide Nanoparticles in the Voltammetric Detection of Heavy Metals: A Review

Simona Sawan<sup>1,2</sup>, Rita Maalouf<sup>2\*</sup>, Abdelhamid Errachid<sup>1</sup>, Nicole Jaffrezic-Renault<sup>1\*</sup>

<sup>1</sup>Institute of Analytical Sciences, University of Lyon, 5 rue de la Doua, 69100 Villeurbanne, France.

<sup>2</sup>Department of Sciences, Faculty of Natural and Applied Sciences, Notre Dame University - Louaize, Zouk Mosbeh, Lebanon

Corresponding authors' email address : [rita.maalouf@ndu.edu.lb](mailto:rita.maalouf@ndu.edu.lb), [nicole.jaffrezic@univ-lyon1.fr](mailto:nicole.jaffrezic@univ-lyon1.fr)

**Keywords :** Heavy metals ; Voltammetry ; Metal nanoparticles ; Metal oxide nanoparticles

## ABSTRACT

Most heavy metal ions are known to be toxic and carcinogenic when present in high amounts. Thus, rapid and reliable on-site detection of these ions is crucial. Voltammetry is a highly sensitive electrochemical method that has been widely used for heavy metal detection offering the advantages of sensitivity and rapidity. On the other hand, nanoparticles offer the advantages of high surface area and high selectivity. Thus, this review aims to highlight the application of metallic and metallic oxide nanoparticles for the voltammetric detection of heavy metals. The nanoparticles used were either applied solely on the electrode or as modifiers with various materials. In all cases, the synthesized devices showed an enhanced analytical performance, such that the limits of detection were lowered and the sensitivities were increased as compared to voltammetric systems not using nanoparticles. Moreover, the applicability of some of these systems was investigated in real samples.

## 1. Introduction

Heavy metals are defined as naturally occurring elements having a density or specific gravity greater than  $5 \text{ g.cm}^{-3}$  and atomic weights between 63.5 and  $200.6 \text{ g.mol}^{-1}$  [1]. Ions of heavy metals, even at trace levels, have been detected in different sources including food, beverages, soil, plants, natural waters, etc. The use of pesticides and fertilizers, burning of fossil fuels, mining, smelting and leaching from eating utensils and cookware are all sources of heavy metal contamination [2, 3]. In addition to human activities, natural sources of heavy metals include: weathering of metal-bearing rocks, volcanic eruptions and forest fires.

Upon their release into the environment, whether through natural or anthropogenic sources, and since they are non-biodegradable, heavy metals accumulate and become toxic when present at high concentrations [4]. They are also known to hinder the developmental activity, yielding capacity and growth of plants. Moreover, heavy metals cause soil pollution and continuous exposure is very harmful to aquatic and terrestrial plants and animals [5]. In addition to their adverse impact on the environment, heavy metals are dangerous to the human health. They enter natural waters and start accumulating in sediments and living organisms, until they reach the final consumers in the food chain, which are human beings [6]. Continued exposure to heavy metals over a prolonged period of time can cause chronic poisoning, growth and developmental abnormalities, nephrotoxicity, encephalopathy, cardiovascular diseases and cancer.

For this reason, for each heavy metal, especially those considered as toxic, several agencies including the World Health Organization (WHO), Environmental Protection Agency (EPA) and Food and Drug Administration (FDA) [7, 8] have set guideline values for the allowable intake and exposure of humans to these heavy metals. Some of these limits are summarized in Table 1.

Table 1: Comparison between the allowable levels of some heavy metals in drinking water following the EPA, WHO and EU guidelines.

Heavy metal	EPA Guideline value in drinkable water ( $\mu\text{g/L}$ )	WHO Guideline value in drinkable water ( $\mu\text{g/L}$ )	EU Guideline value in foodstuff ( $\mu\text{g/Kg}$ )
Antimony	20	5	40
Arsenic	10	10	2
Cadmium	3	3	50
Chromium	50	50	250
Copper	2000	2000	36
Lead	10	10	20
Mercury	6	1	1.6
Nickel	70	20	n/a

Conventional methods that have been used so far for the detection of heavy metals include Inductively Coupled Plasma- Mass Spectrometry (ICP-MS), Liquid Chromatography (LC) [9], UV-vis Spectrometry [10], Atomic Absorption Spectroscopy (AAS), Atomic Emission Spectrometry (AES) [11], Atomic Fluorescence Spectrometry (AFS) [12], Cold Vapor Atomic Fluorescence Spectrometry (CV-AFS) [13], Capillary Electrophoresis (CE) and

50 Laser-Induced Breakdown Spectroscopy (LIBS) [14]. Even though these techniques are highly sensitive and  
51 selective, there still exists several challenges for their use in heavy metal detection [15]. These include high cost,  
52 complex operational procedures, long detection time and difficulty in achieving the detection in real environments  
53 [14].

54 On the other hand, electrochemical methods are gaining wide recognition in heavy metal detection. These  
55 methods offer the same sensitivity with a lower cost, less complex operational procedures and fast on-site detection.  
56 Different electrochemical platforms have been developed for heavy metal detection. Specifically, nanomaterials  
57 have brought several advantages in this area due to their unique electronic, chemical and mechanical properties.  
58 Accordingly, different electrochemical sensors using nanoparticles have been constructed for the detection of heavy  
59 metals [16, 17].

60 To the best of our knowledge, recent reviews focus on the detection of heavy metals using either a specific  
61 technique, or a specific type of nanoparticles [15, 17]. This review mainly discusses the use of voltammetry in the  
62 past fifteen years for heavy metal detection that can be applied to water samples using metal or metal oxide  
63 nanoparticles.  
64

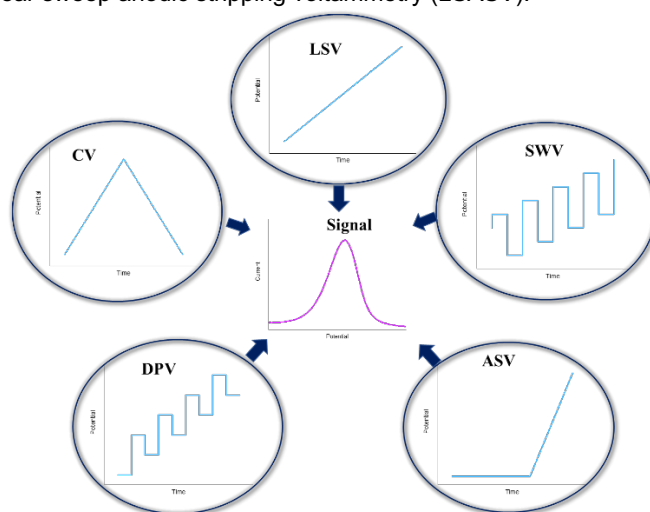
## 65 2. Voltammetric Techniques

66 Among the different known electrochemical methods, voltammetry is the most used in the detection of  
67 heavy metal ions. Voltammetry in general describes all electrochemical systems which are based on potential-  
68 dependent current measurements. A three-electrode electrochemical set-up typically consists of a working  
69 electrode, a counter electrode and a reference electrode. The potential is applied between the working and the  
70 reference electrodes, while the current is measured between the working and the counter electrodes. Upon varying  
71 the method of potential change, one ends up with different techniques. Linear sweep voltammetry (LSV) is the  
72 simplest technique such that the potential is swept linearly with time [18]. Cyclic voltammetry (CV) consists of linearly  
73 scanning the potential in one direction followed by reversing the potential of a working electrode [17]. In other words,  
74 a single or multiple triangular potential waveform [19] are involved.

75 The use of a pulse of voltage signal is the main concept behind pulsed voltammetry. By varying the shape  
76 and amplitude of the pulses, different types of pulsed voltammetry exist [17]. Differential pulse voltammetry (DPV)  
77 uses fixed magnitude pulses superimposed on a linear potential ramp [19]. Square wave voltammetry (SWV) is  
78 when a waveform of a symmetrical square wave is superimposed on a base staircase potential and applied to the  
79 working electrode [19].

80 Stripping voltammetry, and more specifically, anodic stripping voltammetry (ASV) is based on a two-step  
81 process. The first step is a pre-concentration or electrodeposition of the heavy metal at the electrode surface  
82 through the reduction of the metal ions. The second step is the stripping step, where the metal is oxidized back to  
83 give the ion. Having taken the 2 steps into consideration, several factors are known to influence the analysis, such  
84 as electrode material, deposition potential, deposition time [20] ... When the preconcentration step is non-  
85 electrolytic, the analyte accumulates at the surface of the electrode by physical adsorption, a different method is  
86 obtained: Adsorptive Stripping Voltammetry (AdSV) [21]. Figure 1 summarizes how the potential is varied with time  
87 for CV, LSV, DPV, SWV and ASV to produce a signal.

88 A combination of some of these techniques results in increased sensitivities and limits of detection. The  
89 combinations include differential pulse anodic stripping voltammetry (DPASV), square wave anodic stripping  
90 voltammetry (SWASV) and linear sweep anodic stripping voltammetry (LSASV).



91  
92 Figure 1: The graphs of potential vs time for some voltammetry techniques to produce a signal.

### 94 3. Metal Nanoparticles

95 Nanoparticles, specifically metal nanoparticles, present several advantages in the electrochemical sensing  
96 field. Due to their small sizes, nanoparticles can increase the surface area of the electrode being used. Moreover,  
97 metallic nanoparticles can increase the mass-transport rate and offer a fast electron transfer, both increasing the  
98 sensitivity of the used electrodes [16]. In this section, we will present the use of different types of metallic  
99 nanoparticles for the detection of the majority of heavy metals.

100

101

#### 101 3.1. Silver Nanoparticles

102

103

104

105

106

107

108

109

110

111

112

113

114

115

116

117

118

119

120

121

122

123

124

125

126

127

128

129

130

131

132

133

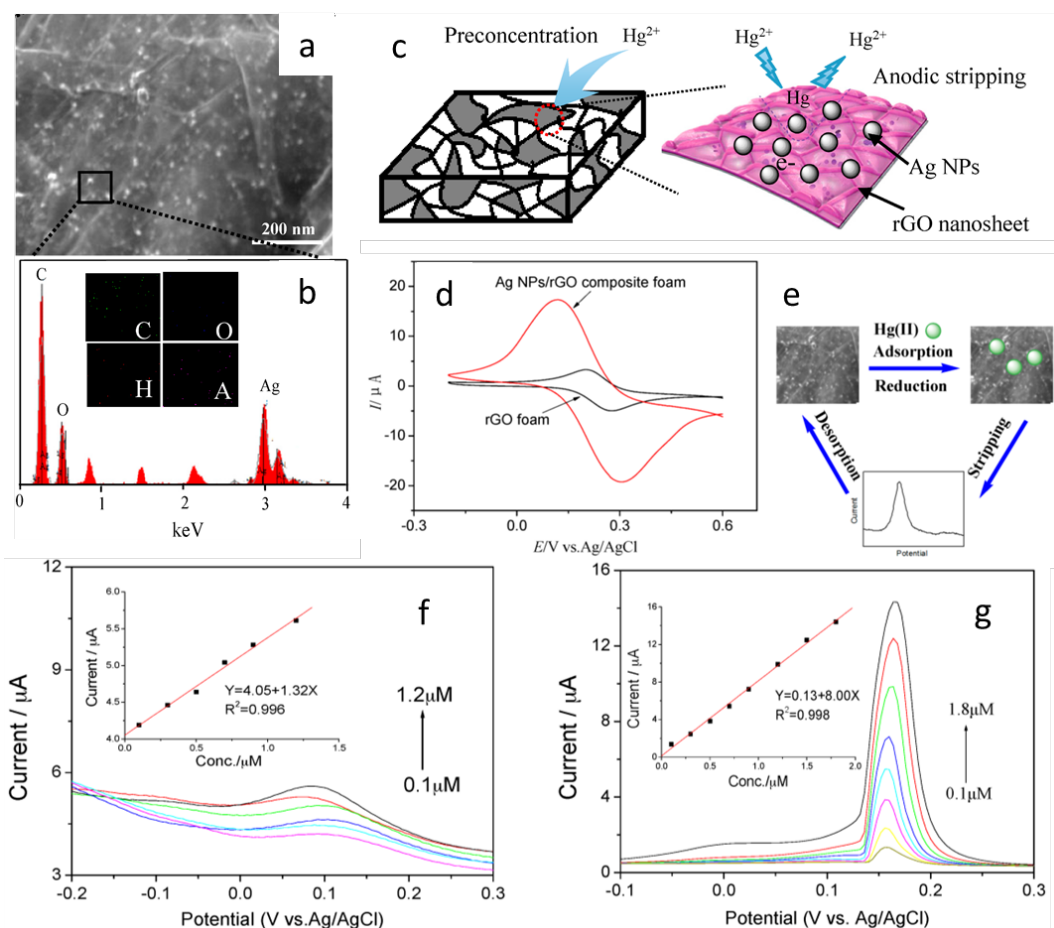
134

135

102 Silver nanoparticles (Ag NPs) are one of the most well-developed nanoparticles because they are relatively  
103 inexpensive and they have unique chemical and physical properties that make them useful in different catalytic,  
104 optical and chemical applications. Silver nanoparticles have been combined with different materials for the detection  
105 of  $\text{Cd}^{2+}$ ,  $\text{Cr}^{6+}$ ,  $\text{Cu}^{2+}$ ,  $\text{Hg}^{2+}$  and  $\text{Sb}^{3+}$ . Two different ways have been employed for the synthesis of spherical Ag NPs:  
106 reduction and electrodeposition. When the NPs were used along with graphene oxide, reduction of silver nitrate  
107 ( $\text{AgNO}_3$ ) was employed, either hydrothermally to produce Ag NPs with an average size of 10 – 20 nm [22] or using  
108 hydrogen iodide HI as a reducing agent to yield Ag NPs with an average particle size of 9.7 nm [23]. The resultant  
109 nanoparticles in both reports were homogeneously distributed on the reduced graphene oxide network. On the other  
110 hand, the electrodeposition of silver nanoparticles [24, 25] produced larger particles with sizes ranging between 30  
111 and 50 nm.

112 Most recently, Cheng et al. synthesized reduced graphene oxide/silver nanoparticles composites for the  
113 simultaneous detection of several ions. Trace levels of  $\text{Cu}^{2+}$ ,  $\text{Cd}^{2+}$  and  $\text{Hg}^{2+}$ , using cyclic voltammetry were detected  
114 with detection limits of  $10^{-15}$  M,  $10^{-21}$  M and  $10^{-29}$  M respectively [22]. Although reporting exceptionally low LODs not  
115 reported elsewhere, specifically for mercury, , this method could detect 1 atom in  $166 \text{ m}^3$  of water! The detection  
116 mechanism is different than all other papers such that it relies on the area of the entirety of the CV curve instead of  
117 using that of a peak. Moreover, the paper lacks important data on the analytical performance such as the linear  
118 range, sensitivity and reproducibility. Han et al. also used silver nanoparticles with reduced graphene oxide to detect  
119  $\text{Hg}^{2+}$  ions by differential square wave anodic stripping voltammetry. The synthesized nanoparticles were spherical  
120 and uniformly distributed on the graphene sheet. The signal and analytical performance were compared with and  
121 without the nanoparticles, and it was shown that the presence of nanoparticles enhanced the signal significantly  
122 (figure 2). A linear concentration range was obtained between 0.1 and  $1.8 \mu\text{M}$ , the limit of detection was calculated  
123 to be  $0.11 \mu\text{M}$  and the sensitivity was  $8 \mu\text{A}/\mu\text{M}$ . Moreover, no interferences were detected from Cd (II) and Cu (II)  
124 [23].

125 Xing et al. modified a glassy carbon electrode with Nafion and electrodeposited silver nanoparticles on its  
126 surface for the direct detection of Cr (VI) using linear sweep voltammetry. A linear range was obtained between 2  
127 and 230 ppb and the limit of detection was 0.67 ppb with no interference from different ions. The applicability of this  
128 sensor was studied using wastewater from a textile factory and the concentration of Cr (VI) was found to be  $6.58 \pm$   
129  $0.04 \mu\text{g}/\text{L}$  with a recovery of  $99 \pm 5\%$  for spiked samples [24]. Renedo et al. also conducted a study using silver  
130 nanoparticles modified screen printed electrodes for the detection of Sb by anodic stripping voltammetry. Differential  
131 pulse anodic stripping voltammetry was used and the linear concentration range was between  $9.9 \times 10^{-8}$  M and  
132  $9.09 \times 10^{-7}$  M, whereas the LOD in case of silver nanoparticles was  $6.79 \times 10^{-10}$  M. Three different seawater samples  
133 were analyzed, and the amount of Sb (III) in all cases was below the detection limit and hence was not detected  
134 [25].



136  
 137 Figure 2: (a) Scanning electron microscopy (SEM) image and (b) energy dispersive spectroscopy (EDS) spectrum  
 138 with elemental mapping of Ag NPs/reduced graphene oxide. (c) Schematic diagram of the Ag NPs/reduced  
 139 graphene oxide structure. (d) Cyclic voltammetry of pure reduced graphene oxide and Ag NPs/reduced graphene  
 140 oxide. (e) Schematic representation of the electrochemical detection towards Hg (II) ions. (f) and (g) SWASV  
 141 response of pure reduced graphene oxide and Ag NPs/reduced graphene oxide towards Hg (II) at different  
 142 concentrations in a 0.1 M NH<sub>3</sub> solution; the insets correspond to the calibration plots, respectively [23].  
 143

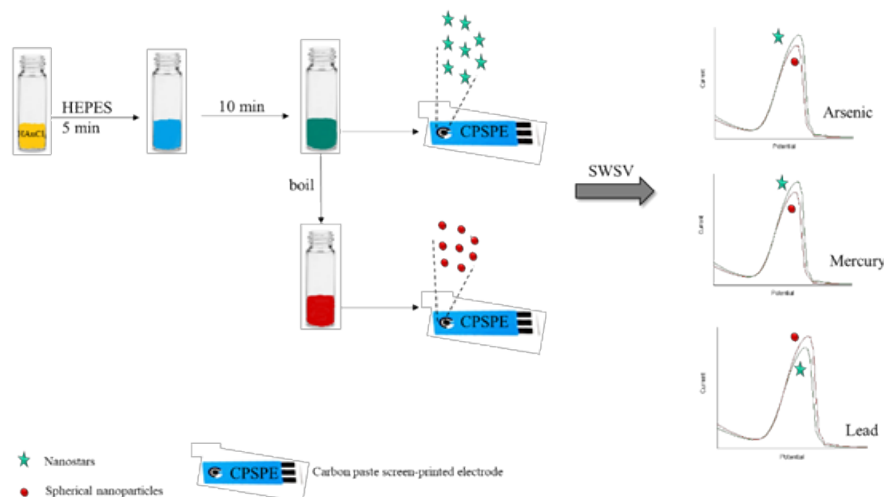
### 144 3.2. Gold Nanoparticles

145 The most used nanoparticles for the electrochemical detection of heavy metals are gold nanoparticles (Au  
 146 NPs). Their properties vary depending on their size, but whatever the size, gold nanoparticles are known to be  
 147 biocompatible and of low toxicity [26]. Table 2 summarizes the different voltammetric studies done to detect heavy  
 148 metals using gold nanoparticles. Only a few reports focus on the use of gold nanoparticles alone; nonetheless,  
 149 different materials have been associated with gold nanoparticles for the detection of heavy metals, and especially  
 150 mercury and lead.

151 Similar to Ag NPs, the most common methods utilized for the synthesis of Au NPs are either  
 152 electrodeposition or reduction. However, different synthesis conditions lead to different shapes and sizes of the gold  
 153 nanoparticles. The most common shape used in the electrochemical detection of heavy metals is spherical. Most  
 154 groups have successfully synthesized spherical Au NPs of sizes ranging between 4 and 298 nm. Hassan et al.  
 155 reported the synthesis and use of different gold nanostructures for the detection of As (III). The synthesis involved  
 156 the reduction of chloroauric acid using ibuprofen in a basic medium. They investigated the effect of different heating  
 157 times on the shape of the produced nanoparticles, and the results indicated that with increased heating time,  
 158 nanoflowers formed along with other structures [27]. Ouyang et al. used a more complex method for the synthesis  
 159 of nanoflowers. In brief, they modified a glassy carbon electrode with a layer of gold nanoparticles, followed by a  
 160 layer of 3-mercaptopropyl-trimethoxysilane. Then, the electrode was immersed in a solution containing Au NPs to  
 161 form a second layer of nanoparticles and pyridinium was attached to the NPs after dipping in 4-pyridineethanethiol  
 162 hydrochloride solution [28]. Dutta et al. synthesized gold nanostars and spherical gold nanoparticles and compared  
 163 their performances in the detection of As (III), Hg (II) and Pb (II). The nanostars were prepared by mixing an auric  
 164 chloride solution with 4-(2-hydroxyethyl)-l-piperazineethanesulfonic acid (HEPES) without stirring or shaking.  
 165 Boiling the resultant nanostars for 5 minutes yielded spherical nanoparticles. Using these 2 structures, they modified  
 166 a screen-printed electrode and optimized some conditions to conclude that the gold nanostar shape improved the

167 detection of arsenic compared to the spherical shape (figure 3) [29]. Later on, different studies used the same  
 168 procedure for the gold nanostars synthesis to detect Cr (II), Cd (II), As (III) and Se (IV) [30, 31].

169 It is worthy to note that the use of gold nanoparticles associated with different sensors is gaining wide  
 170 recognition. Even though the inhibition of enzymatic activity by heavy metals has been extensively studied, only  
 171 one study uses enzyme-based biosensors with gold nanoparticles to detect mercury ions. The presence of gold  
 172 nanoparticles considerably increased the analytical response [32]. Some researchers focus on the use of gold  
 173 nanoparticles with amino acid- based biosensors. Amino acids and peptides (amino acid chains) have a high affinity  
 174 towards some heavy metals which can be tuned by altering the peptide sequence [33]. Amino acids are known to  
 175 bind heavy metal ions through cooperative metal-ligand interactions [34]. The use of gold nanoparticles with these  
 176 biosensors amplifies the signal, improving the analytical performance [35]. The majority of authors focus on DNA-  
 177 based biosensors with an emphasis on certain interactions between the DNA bases and certain heavy metal ions.  
 178 Specifically, silver ion and mercury ion are well known to interact with cytosine-cytosine mismatch and thymine-  
 179 thymine mismatch, respectively, to form stable base pairs [36 – 40].



180

181 Figure 3: Modification of carbon paste screen-printed electrodes by Au NPs for the detection of As<sup>3+</sup>,  
 182 Hg<sup>2+</sup> and Pb<sup>2+</sup> [29].

183 Table 2: Comparison between the different studies using gold nanoparticles for heavy metal detection.

HM	Technique	Electrode	LOD (μM)	Sensitivity (μA/μM)	Linear range (μM)	Addition to Au NPs	Real sample	Ref
Ag <sup>+</sup>	DPV	Au	3×10 <sup>-5</sup>	124.6	10 <sup>-4</sup> – 0.12	Oligonucleotide sequences		36
As <sup>3+</sup>	SWV	GCE	10 <sup>-3</sup>	71.7			River water	41
	SWV	GCE	8.89×10 <sup>-4</sup>	1985		Multiwalled Carbon nanotubes		42
	ASV	CμF	67.43	1318	0.067 – 0.8		Tap, well water	43
	SWASV	GNEE	1.78×10 <sup>-4</sup>	0.7492	0 – 0.2	3-(mercaptopropyl)trimethoxy silane		44
	SWASV	SPE	6.53×10 <sup>-3</sup>				River water	31
	SWASV	GCE	1.06×10 <sup>-3</sup>	113.9	0.01 – 0.67			45
	SWASV	SPE	0.01		0.03 – 10.2		Ground water	29
	LSV	GCE	0.024		0 – 1.2			47
	LSV	GCE	5.34×10 <sup>-3</sup>	32.8		Multiwalled Carbon nanotubes		42
	LSV	GCE	2×10 <sup>-3</sup>	14.2			River water	41
LSASV	GCME	0.01		0.01 – 10.01	Carbon nanotube		48	
LSASV	GCE	3.7×10 <sup>-3</sup>	940	0.005 – 3	Pt NPs	Tap, spring, river water	49	
LSASV	GCE	2.9×10 <sup>-3</sup>	230	0.005 – 1	Porous graphitic carbon nitride	Tap, spring, river water	50	
DPV	GCE	0.2	0.8075	4 – 40	Crystal violet	Drinking water	51	

	DPSV	SPCE	$8.01 \times 10^{-4}$		Up to 53.4	Poly(L-lactide)	Ground, surface water	52
	CV	Basal-plane pyrolytic graphite	0.8			Glassy carbon microsphere		53
	CV	SPCE	$2.4 \times 10^{-4}$		$1.3 \times 10^{-3} - 24$	Ibuprofen	Drinking, tap, river, ground water	27
<b>Cd<sup>2+</sup></b>	DPV	SPCE	0.023	26.19	0.07 – 4448		River, tap water	54
	DPV	GCE	0.022		0.05 – 300	Reduced graphene oxide, Tetraphenylporphyrin	Lake water	55
	DPASV	GCE	0.3	3.24	0 – 1.4			56
	SWV	GCE	$8.89 \times 10^{-4}$		$4.4 \times 10^{-3} - 0.35$	Graphene, cysteine	Spring water	35
	SWASV	GCE	0.1	1.88	0.1 – 1	Carbon nanofibers		57
	SWASV	SPE	0.015				River water	31
	SWASV	GCE	$6 \times 10^{-5}$	$2.2 \times 10^3$	$10^{-3} - 0.01$	L-cysteine, reduced graphene oxide	Lake, tap, sewage, ground water	58
<b>Cr<sup>3+</sup></b>	SWV	GCE			100 – 400			59
<b>Cr<sup>6+</sup></b>	SWV	SPE	0.096		0.19 – 96		River water	60
	SWV	GCE	$1.92 \times 10^{-4}$	5.98	$2.5 \times 10^{-3} - 0.86$		Sewage, tap water	61
	SWCSV	GCE	$5.58 \times 10^{-5}$		$1.9 \times 10^{-4} - 23$	3-mercaptopropyl-trimethoxysilane		28
	AdSV	Graphene	0.02	$1.94 \times 10^{-4}$	0.48 – 5.77	Reduced graphene oxide, 4-pyridylethylmercaptan hydrochloride	Waste water	73
	DPV	SPCE	0.4	$2.01 \times 10^{-8}$	0.4 – 30		Tap, sea water	74
	CV	Indium tin oxide	2	0.3025	5 – 100		Tap, sea, stream water	75
	LSV	SPE	0.067		0.19 - 1442		Ground water	30
<b>Cu<sup>2+</sup></b>	LSV	SPCE	0.1	0.0572	0.38 – 3.8		River water	76
	DPV	SPCE	0.126		0.79 – 157	L-cysteine		33
	DPASV	GCE	0.3	4.18	0 – 1.4			56
	ASV	GCE	$5 \times 10^{-5}$	3690	Logarithmic	Graphene quantum dots, cysteamine		68
	SWV	Au	$10^{-7}$	$0.29435 \times 10^{-6}$	$10^{-4} - 10$	4-aminothiophenol, DNAzymes	Lake, tap water	37
	SWASV	SPE	0.025	4.368	0.31 – 4.72			70
	SWASV	GNEE	$2.22 \times 10^{-3}$		$6.67 \times 10^{-3} - 0.2$	3-(mercaptopropyl)trimethoxy silane		44
<b>Hg<sup>2+</sup></b>	SWASV	GCE	0.1	4.41	0.1 – 1	Carbon nanofibers		57
	SWASV	GNEE	$9.97 \times 10^{-5}$	2.006	0 – 0.07	3-(mercaptopropyl)trimethoxy silane		44
	SWASV	SPE	$2.49 \times 10^{-3}$		$7.5 \times 10^{-3} - 2.69$		Ground water	29
	SWASV	GCE	$2.99 \times 10^{-5}$	708.3 7.37	$3.99 \times 10^{-5} - 2.49 \times 10^{-4}$ $4.98 \times 10^{-4} - 0.3$	Chitosan graphene	River water	77
	SWASV	SPCE	$3.99 \times 10^{-3}$		$2.49 \times 10^{-5} - 10^{-4}$		Rain, river water	78
	SWASV	GCE	$4.2 \times 10^{-4}$	1370	$0.64 \times 10^{-3} - 4 \times 10^{-3}$			79

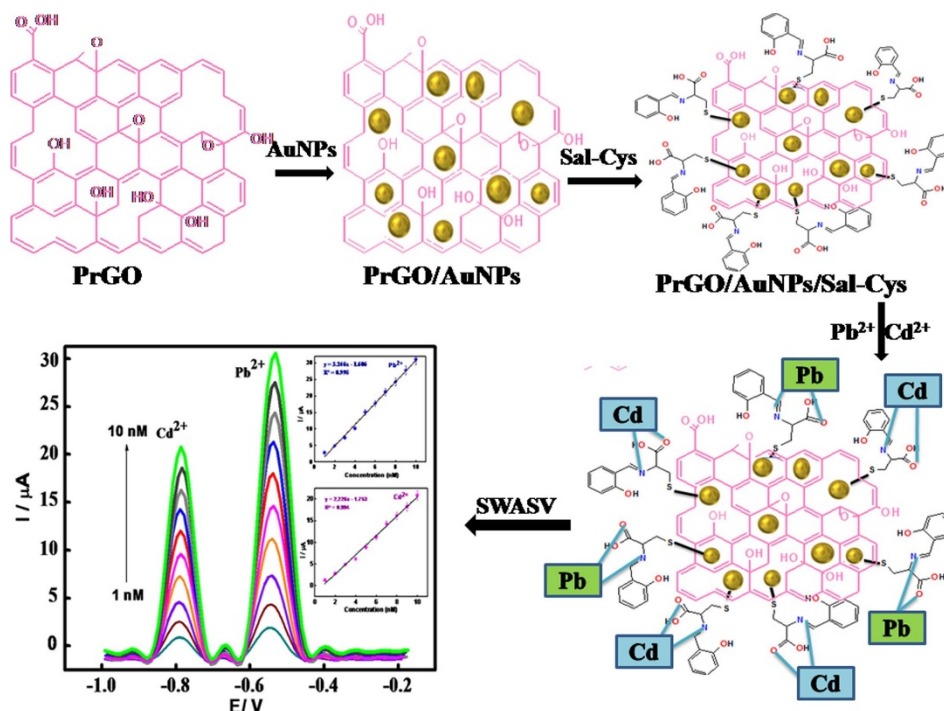
	SWASV	Pencil graphite	$4 \times 10^{-15}$		$10^{-13} - 10^{-4}$	DNA, L-methionine	Sea water, fish	80
	SWV	Au	$5 \times 10^{-4}$		0.09-1.99	MSO, linker probes		81
	SWV	Carbon ionic liquid	$2.3 \times 10^{-3}$		0.01 – 20	Thiolated amino acids	Waste, tap water	34
	SWV	SPE	$9.97 \times 10^{-4}$	47.54	$2.5 \times 10^{-3} - 0.25$	Carbon nanotubes	Tap, river water	71
	DPV	GCE	$3 \times 10^{-5}$	35.88	$10^{-4} - 0.02$	Multi-walled C nanotubes, DNA	Tap, lake water	39
	DPV	GCE	$7.48 \times 10^{-6}$	1603.6	$4.98 \times 10^{-5} - 4.98 \times 10^{-3}$	Reduced graphene oxide, thymine-1-acetic acid, cysteamine	Tap water	62
	DPV	Au	$5 \times 10^{-4}$		$10^{-3} - 0.1$	DNA, methylene blue	Tap, river water	38
	DPV	Indium tin oxide	$7.8 \times 10^{-4}$		$5 \times 10^{-3} - 0.11$	Graphene oxide, 5-methyl-2-thiouracil	Tap, lake, bottled water	63
	DPV	Au	$7.38 \times 10^{-6}$	333	$5 \times 10^{-5} - 2.5 \times 10^{-3}$	Thiolated probe DNA	Tap water	40
	DPASV	GCE	$8 \times 10^{-5}$	749	$4 \times 10^{-4} - 0.096$	Single walled C nanotubes, poly(2-mercaptobenzothiazole)	River, tap water	65
	DPASV	GCE	0.3	3.39	0 – 1.4			56
	DPASV	GCE	$10^{-4}$	0.09	$5 \times 10^{-4} - 1.25$	Carbon nanotubes		82
	DPASV	Indium tin oxide	$1.49 \times 10^{-4}$		$4.98 \times 10^{-4} - 0.05$		Tap, lake water, milk, soil	66
	ASV	GCE	0.16		0.79 – 3.15		River water	77
	ASV	GCE	$7.48 \times 10^{-7}$		Up to 0.25		Drinking water	67
	ASV	GCE	$2 \times 10^{-5}$	2470	$2 \times 10^{-5} - 0.1$	Graphene quantum dots, cysteamine		68
	CV	Au	0.01			MSO, ss-DNA		69
<b>Pb<sup>2+</sup></b>	SWASV	GCE	$4 \times 10^{-5}$	$3.2 \times 10^3$	$10^{-3} - 0.01$	L-cysteine, reduced graphene oxide	Lake, tap, sewage, ground water	58
	SWASV	SPE	0.02		0.06 – 1.56		Ground water	29
	SWASV	SPE	0.0106	31.91	0.096 – 0.96			70
	SWASV	GCE	0.1	19.08	0.1 – 1	Carbon nanofibers		57
	SWV	SPE	$4.34 \times 10^{-4}$	17.612	0.01 – 1.2		Tap, river water	71
	SWV	GCE	$2.4 \times 10^{-4}$		$2.41 \times 10^{-3} - 0.19$	Graphene, cysteine	Spring water	72
	SWV	GCE	800	455.83	0.01 – 0.15	Graphene oxide	Tap water	83
	CV	Au	$2.8 \times 10^{-5}$			DNA		32
	DPASV	GCE	0.3	17.63	0 – 1.4			56
	DPASV	GCE	$4.83 \times 10^{-5}$	24.86	$2.41 \times 10^{-3} - 0.48$	Graphene oxide, chitosan	River water	84
	DPV	Au	$10^{-3}$		$5 \times 10^{-3} - 0.1$	DNAzymes		64
	DPV	GCE	$4.3 \times 10^{-9}$		$10^{-8} - 5 \times 10^{-5}$	Multi-walled carbon nanotubes, DNA	Tap, river, spring water	85
<b>Sb<sup>3+</sup></b>	DPASV	SPE	$9.44 \times 10^{-4}$		$9.9 \times 10^{-2} - 0.909$		Sea water, drugs	86
<b>Se<sup>4+</sup></b>	SWASV	SPE	0.01				River water	31

184 Abbreviations: Au gold, GCE glassy carbon electrode, C<sub>μ</sub>F carbon ultra-microfiber, GNEE gold nanoelectrode  
185 ensembles, SPE screen printed electrode, GCME carbon nanotube flow-through membrane electrode, SPCE  
186 screen printed carbon electrode.

187 From the above table, it can be concluded that the best analytical performance for the detection of As (III)  
188 is obtained using gold nanoparticles modified carbon nanotubes [42]. The process of electrode modification and  
189 arsenic detection using square wave voltammetry can be achieved within minutes producing a very high sensitivity  
190 and low LOD compared to similar studies. Although the authors claim that this sensor can be used for the detection  
191 of arsenic in natural waters, to the best of our knowledge, the study has not been conducted. The modification of a  
192 glassy carbon electrode with gold nanoparticles, L-cysteine and reduced graphene oxide showed a superior



193 performance in the detection of Cd (II) by square wave voltammetry (figure 4). The modified electrode was used to  
 194 assess the concentrations of cadmium in different water sources (lake, sewage, tap and ground water) and the  
 195 obtained results were comparable with those of AAS [58]. The same electrode exhibited the highest reported  
 196 sensitivity for the detection of Pb (II) as well; however, a better LOD was obtained by Zhu et al. [85] using differential  
 197 pulse voltammetry. The latter team modified a glassy carbon electrode with gold nanoparticles, cysteine, graphene  
 198 and bismuth film which exhibited a low LOD and good repeatability and reproducibility along with the possible usage  
 199 in real water samples such as spring water. However, the preparation procedure was too complex compared with  
 200 other studies. The modification of a GCE with graphene quantum dots and Au NPs is the method of choice for the  
 201 detection of Cu (II) using anodic stripping voltammetry. Both the LOD and sensitivity are better than those obtained  
 202 with different modifications, unfortunately the electrode was not tested with real samples [68]. This same electrode  
 203 showed the highest sensitivity for the detection of Hg (II), while an outstanding LOD was obtained by Hasanjani et  
 204 al. [80] who used DNA and L-methionine along with Au NPs for the modification of a pencil graphite electrode.  
 205 Interestingly, for the detection of Cr (VI), the sensitivities are either not reported, or are very small, with the best  
 206 limit of detection obtained by Ouyang et al. [28] who modified a glassy carbon electrode with Au NPs and 3-  
 207 mercaptopropyltrimethoxysilane. It should be noted that the focus of most of the papers using gold nanoparticles  
 208 was on the synthesis of the nanoparticles and not on testing the applicability of the sensor in real samples. However,  
 209 it was implied in some of the studies that their fabricated sensors can be used in real samples.



210  
 211 Figure 4: Schematic diagram of the possible interactions of Cd (II) and Pb (II) with gold nanoparticles, L-cysteine  
 212 and reduced graphene oxide modified GCE electrode leading to the simultaneous analysis of the heavy metals [58].  
 213 Reproduced with permission from Elsevier

### 214 3.3. Bismuth Nanoparticles

215 The use of bismuth in different areas of chemistry (catalysis, organic synthesis, clusters...) has grown in  
 216 the past decade. In electroanalytical chemistry, bismuth is used as an electrode coating, replacing the mercury  
 217 electrode, because of its low toxicity and excellent peak resolution.

218 Lee et al. used bismuth nanopowder modified electrode to detect Zn, Cd and Pb ions using square wave  
 219 anodic stripping voltammetry. Spherical bismuth was prepared with different particle size distribution in order to  
 220 investigate its effect on the sensitivity and limit of detection of the studied metals. It was concluded that as the  
 221 particle size decreases from 406 to 166 nm, both the sensitivity and the limit of detection are improved [87]. In  
 222 another work, the same group modified a thick-film graphite electrode with bismuth nanopowder for the detection  
 223 of thallium (Tl). Applying the same procedure, a limit of detection of 0.03 μg/L was obtained with the possibility to  
 224 overcome any interference from divalent ions through the addition of EDTA [88]. Rico et al. [89] adopted the method  
 225 of Lee et al. [87], to modify a screen-printed carbon electrode and detect the heavy metals. Optimization of the  
 226 method included the accumulation configuration; both convective and flow configurations were tested. The limits of  
 227 detection that were obtained at the flow cell for Zn (II), Cd (II) and Pb (II) were better than those at the convective  
 228 cell. Those limits were 2.6, 1.3 and 0.9 ng/mL, respectively. Moreover, the reproducibility and sensitivity of the  
 229 method were good after analyzing a certified reference sample and tap water, but further tests showed that high  
 230 concentrations of Cu (II) interfered with the results. Saturno et al. modified a glassy carbon electrode with micro-  
 231 nanoparticles/bismuth film for the determination of cadmium and lead by differential pulse voltammetry. The shape

232 and size of the nanoparticles were irregular, but they still obtained LODs of 11  $\mu\text{g/L}$  for Cd (II) and 18  $\mu\text{g/L}$  for Pb  
233 (II) with the response being highly reproducible [90]. Sahoo et al. modified a carbon paste electrode with graphene  
234 oxide and bismuth nanoparticles of diameter between 40 and 100 nm for the determination of zinc, cadmium, lead  
235 and copper ions using differential pulse anodic stripping voltammetry. A linear concentration range was obtained  
236 from 20 to 120  $\mu\text{g/L}$  with limits of detection of 2.8, 0.55, 17 and 26  $\mu\text{g/L}$  for  $\text{Cd}^{2+}$ ,  $\text{Pb}^{2+}$ ,  $\text{Zn}^{2+}$  and  $\text{Cu}^{2+}$ , respectively.  
237 The performance of the electrode was tested in two different water samples, ground and lake water, and the  
238 concentrations of the divalent metals were determined [91]. The obtained LODs were comparable in the different  
239 studies for lead and cadmium ions. However, the problem of Cu (II) interference was faced in more than one study.  
240

#### 241 3.4. Platinum Nanoparticles

242 Platinum metal has received a lot of attention in the catalysis industry. Platinum nanoparticles (Pt NPs)  
243 have also found a lot of applications in electrochemical analyses due to their stability and conductivity [92]. Hrapovic  
244 et al. electrodeposited spherical platinum nanoparticles on a glassy carbon electrode and on a boron doped  
245 diamond electrode for the detection of Arsenite (As (III)). The electrodeposition resulted in a non-homogenous and  
246 non-uniform distribution of the Pt NPs. Using linear sweep voltammetry, the boron-doped electrode was proven to  
247 have a superior performance with a limit of detection of 0.5 ppb without interference from copper (II) ions. Moreover,  
248 the analysis of drinking water and river water from Montreal confirmed that As (III) concentrations can be determined  
249 without any interference [93]. Spherical platinum nanoparticles of diameters between 105 and 180 nm were also  
250 electrodeposited on a glassy carbon electrode by Dai et al. for the detection of Arsenic (III) ions. Cyclic voltammetry  
251 was applied and the measured limit of detection was 35 ppb. The performance of this electrode was compared  
252 using different techniques (square wave voltammetry and differential pulse voltammetry) all giving the same results.  
253 Moreover, possible interfering ions were investigated and the results still showed a clear peak for arsenic [94]. Both  
254 studies rely on the oxidation of As (III) to As (V) electrocatalyzed by Pt on a BDD electrode. Dai et al. obtained a  
255 LOD that is higher than recommended guidelines for water. Moreover, even though Hrapovic et al. obtained a lower  
256 LOD, the electrodeposited Pt NPs were not uniform in size.  
257

#### 258 3.5. Other metal nanoparticles

259 Owing to the advantages of nanoparticles in the modification of electrodes in electrochemical analysis,  
260 different metal nanoparticles have been used for the electrochemical detection of cadmium, copper, mercury and  
261 lead.

262 Two groups have reported the use of palladium nanoparticles (Pd NPs) for the detection of heavy metals.  
263 Both groups synthesized porous activated carbon (PAC), followed by the decoration of PAC with palladium  
264 nanoparticles via a one-step thermal reduction method (with slightly different conditions). Spherical 20 – 30 nm Pd  
265 NPs were used by Zhang et al. for the simultaneous and individual determination of  $\text{Cd}^{2+}$ ,  $\text{Pb}^{2+}$  and  $\text{Cu}^{2+}$  by applying  
266 square wave anodic stripping voltammetry (figure 5). The obtained limits of detection for individual determinations  
267 were 13.33, 6.6 and 11.92 nM for  $\text{Cd}^{2+}$ ,  $\text{Pb}^{2+}$  and  $\text{Cu}^{2+}$ , while for simultaneous determinations the values were 20.9,  
268 9.19 and 14.78 nM, respectively. The applicability of the sensor was successfully tested in practical water, without  
269 specifying what this water is. [95]. Veerakumar et al. were able to obtain smaller crystals with an average size of 4  
270 – 5 nm. They used differential pulse voltammetry for the detection of  $\text{Cd}^{2+}$ ,  $\text{Pb}^{2+}$ ,  $\text{Cu}^{2+}$  and  $\text{Hg}^{2+}$ . Results showed  
271 superior performance for both individual and simultaneous detections. For simultaneous detection of  $\text{Cd}^{2+}$ ,  $\text{Pb}^{2+}$ ,  
272  $\text{Cu}^{2+}$  and  $\text{Hg}^{2+}$ , a linear response in the ion concentration ranges of 0.5 – 5.5, 0.5 – 8.9, 0.5 – 5.0 and 0.24 – 7.5  
273  $\mu\text{M}$ , with sensitivities of 66.7, 53.8, 41.1 and 50.3  $\mu\text{A } \mu\text{M}^{-1} \cdot \text{cm}^{-2}$ , and detection limits of 41, 50, 66 and 54 nM,  
274 respectively, were observed [96].

275 Lee et al. have used tin nanoparticles (Sn NPs) with reduced graphene oxide on glassy carbon electrode  
276 for the determination of  $\text{Cd}^{2+}$ ,  $\text{Pb}^{2+}$  and  $\text{Cu}^{2+}$ . The Sn NPs of 50 nm diameter were synthesized using the  
277 electrochemical reduction of  $\text{Sn}^{2+}$  with graphene oxide solution. Individual analysis of metal ions using square wave  
278 anodic stripping voltammetry showed a high stability and detection limits of 0.63 nM, 0.60 nM and 0.52 nM,  
279 respectively. However, simultaneous analysis of the heavy metal increased the detection limits to 7.56 nM, 6.77 nM  
280 and 5.62 nM, respectively due to the possible formation of intermetallic compounds. The feasibility of the sensor  
281 was tested in tap water samples with and without spiking. No peaks were observed before spiking, while recoveries  
282 ranged between 97 and 102% after spiking [97].

283 Toghiani et al. modified a BDD electrode with Sb nanoparticles for the detection of  $\text{Cd}^{2+}$  and  $\text{Pb}^{2+}$  using linear  
284 sweep anodic stripping voltammetry. The nanoparticles were electrochemically deposited on the electrode, with an  
285 average size of  $108 \pm 70$  nm, but due to the toxicity of Sb, the team tried to use the smallest possible concentration  
286 of antimony. Based on this study, the addition of Sb nanoparticles didn't improve the individual detection of each  
287 analyte as compared to the bare BDD. On the other hand, simultaneous detection of cadmium and lead was  
288 improved and Pb did not inhibit Cd from nucleating on the electrode surface like previous works [98].

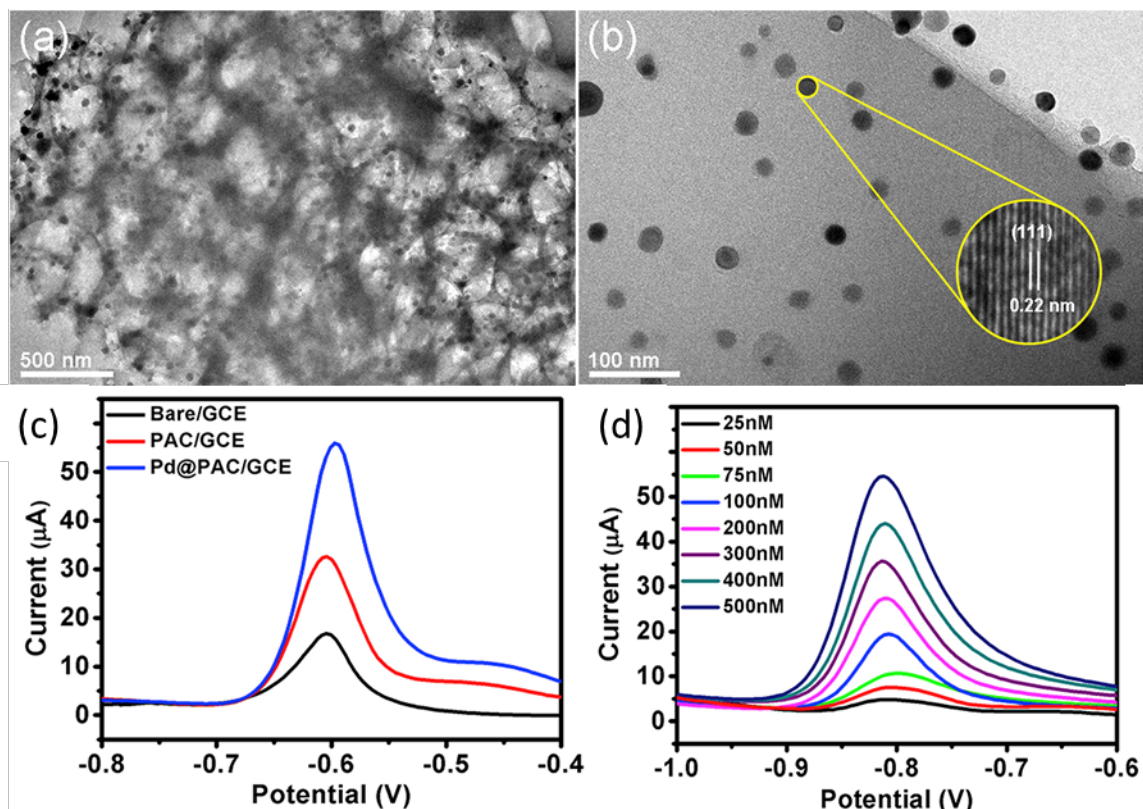


Figure 5: (a) and (b) TEM and HR-TEM images of Pd@Pac. (c) SWASV curves for 500 nM each of Cd<sup>2+</sup>, Pb<sup>2+</sup> and Cu<sup>2+</sup> on the bare, PAC-modified and Pd@PAC-modified GCEs in 0.1 M acetate buffer solution (pH 4.8). Conditions: deposition potential: 2.1 V; deposition time: 210 s; room temperature; amplitude: 50 mV; increment potential: 4 mV; and frequency: 15 Hz. (d) SWASV curves of the Pd@PAC/GCE for the individual analysis of Cd<sup>2+</sup> [95]. Reproduced with permission from Elsevier

289  
290  
291  
292  
293  
294  
295

#### 4. Metal oxide nanoparticles

Metal oxide nanoparticles are being extensively studied in electrochemical detection these past few years. They have been synthesized using different methods to obtain different sizes, stability, and morphology. These differences allow them to exhibit various electrical and photochemical properties resulting in different applications [99]. Various oxides of metals, mainly transition metals, have been used in the modification of electrodes for the detection of different analytes including heavy metals. Even though these oxides have been synthesized using almost all transition metals, only a few were used for the detection of heavy metals.

296  
297  
298  
299  
300  
301  
302

##### 4.1. Iron oxide Nanoparticles

The most common metal oxide used for the detection of heavy metals is iron oxide in different forms (MnFe<sub>2</sub>O<sub>4</sub>, Fe<sub>2</sub>O<sub>3</sub> and Fe<sub>3</sub>O<sub>4</sub>). While iron in the first 2 species is found as Fe<sup>3+</sup>, both Fe<sup>2+</sup> and Fe<sup>3+</sup> are present in Fe<sub>3</sub>O<sub>4</sub>, which permits an electron hopping process between the 2 ions, and thus increasing the electrical conductivity compared to MnFe<sub>2</sub>O<sub>4</sub> and Fe<sub>2</sub>O<sub>3</sub>.

303  
304  
305  
306  
307

Lee et al. were the first group to report the use of iron oxide in the form of Fe<sub>2</sub>O<sub>3</sub>. Briefly, graphene oxide was prepared and reduced, after which Fe<sub>2</sub>O<sub>3</sub>/graphene composites were prepared using a solvent-less method by mixing iron (III) acetylacetonate and oleic acid with the prepared graphene. The synthesized spherical maghemite nanoparticles had an average size of 30 nm and uniformly decorated the graphene sheets. Prior to be used in the detection of Pb<sup>2+</sup>, Zn<sup>2+</sup> and Cd<sup>2+</sup> in tap water, the nanoparticles with graphene oxide were deposited on a cleaned glassy carbon electrode and dried under infrared heat lamp, and the electrode was modified with bismuth. Differential pulse anodic stripping voltammetry was applied and the analysis showed a linear range of detection between 1 and 100 μg.L<sup>-1</sup> for all the ions, and limits of detection of 0.11 μg.L<sup>-1</sup> for Zn (II), 0.08 μg.L<sup>-1</sup> for Cd (II) and 0.07 μg.L<sup>-1</sup> for Pb (II) [100]. Li et al. later reported the synthesis of 2 different morphologies (nanorods and nanocubes) of Fe<sub>2</sub>O<sub>3</sub> for the electroanalysis of Pb (II) by anodic stripping voltammetry. The limit of detection of Pb (II) by nanorods was much smaller (0.0034 μM) than that with nanocubes (0.083 μM). Moreover, Fe<sub>2</sub>O<sub>3</sub> nanorods proved to be much more sensitive (109.67 μA.μM<sup>-1</sup>) compared to nanocubes (17.68 μA.μM<sup>-1</sup>). The practicability of the proposed sensor was evaluated in drinking water, and good recoveries were observed with a slightly decreased sensitivity for lead that could be the result of interfering ions [101].

308  
309  
310  
311  
312  
313  
314  
315  
316  
317  
318  
319  
320  
321

On the other hand, Fe<sub>3</sub>O<sub>4</sub> is the most common form of iron oxide used to detect heavy metals. Most recently, Fe<sub>3</sub>O<sub>4</sub> nanoparticles have been investigated for heavy metal detection. Fe<sub>3</sub>O<sub>4</sub> is known for having a high

322  
323

324 affinity for heavy metal ions, but only a few reports that use iron oxide alone are available. This is due to the fact  
 325 that iron oxide nanoparticles have the tendency to aggregate and become non-conductive units [102]. Most studies  
 326 use either functionalized Fe<sub>3</sub>O<sub>4</sub> or Fe<sub>3</sub>O<sub>4</sub> combined with other materials. Table 3 summarizes the different studies  
 327 done using Fe<sub>3</sub>O<sub>4</sub> to detect heavy metals. Most of the magnetic nanoparticles used in heavy metal detection were  
 328 spherical or quasi-spherical with sizes ranging between 5.8 nm and 200 nm. Sun et al. synthesized different Fe<sub>3</sub>O<sub>4</sub>  
 329 shapes by varying the ratio of Fe<sup>2+</sup> to Fe<sup>3+</sup> ions. They used a one-step coprecipitation method with the following  
 330 molar ratios of Fe<sup>2+</sup>/Fe<sup>3+</sup>: 2/5 to obtain spherical nanoparticles, 4/0 to get rod Fe<sub>3</sub>O<sub>4</sub> (20 – 50 nm in width and 200  
 331 – 300 nm in length) and 5/4 to obtain band Fe<sub>3</sub>O<sub>4</sub> (80 – 120 nm in width and 300 – 400 nm in length) (Figure 6).  
 332 Along with reduced graphene oxide, the iron oxide nanoparticles were used for the detection of Pb (II) and it was  
 333 shown that the sensitivity is best with the band nanoparticles followed by spherical nanoparticles and then rod  
 334 nanoparticles (the results are shown in decreasing order in Table 3). On the other hand, the limit of detection did  
 335 not differ much between the three structures. Band NPs were also used for the detection of Cu (II) and Cd (II) [103].

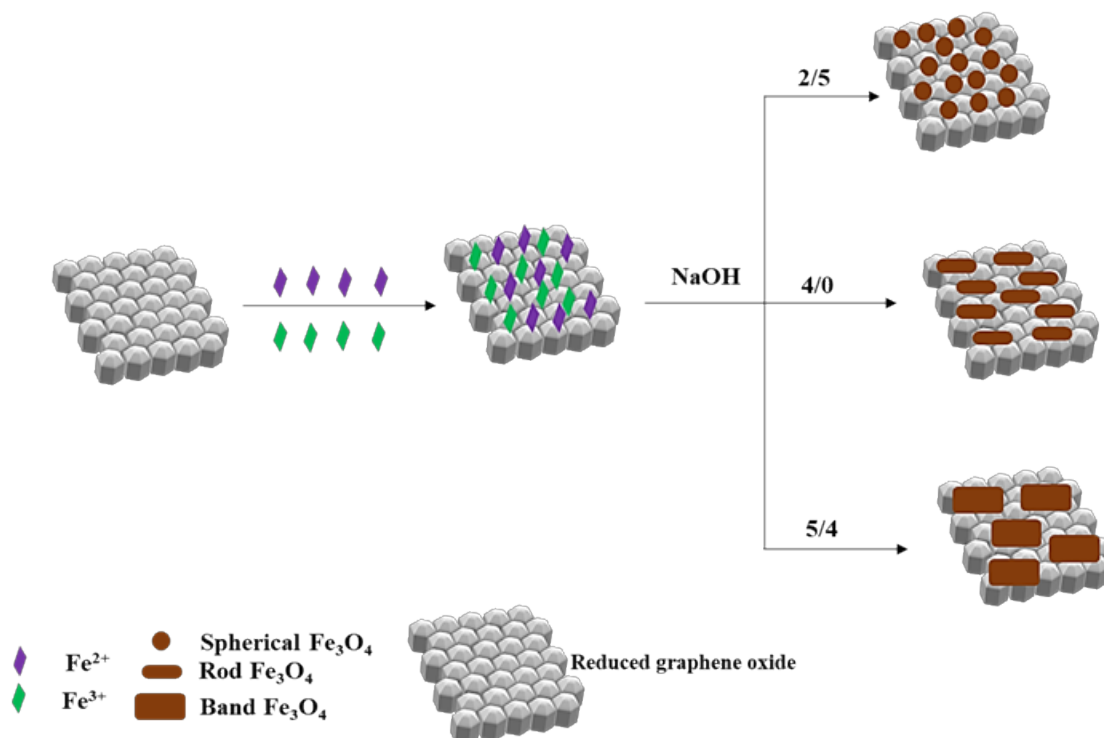


Figure 6: Synthesis of Fe<sub>3</sub>O<sub>4</sub> nanoparticles, nanorods and nanobands done by Sun et al. [103]

339 Table 3: Comparison between the different studies using Fe<sub>3</sub>O<sub>4</sub> to detect heavy metals.

HM	Technique	Electrode	LOD (μM)	Sensitivity (μA/μM)	Linear range (μM)	Addition to iron oxide NPs	Real sample	Ref
Pb <sup>2+</sup>	SWV	GCE	2.41×10 <sup>-4</sup>		0 – 0.24	DMSA	Urine	104
Ag <sup>+</sup> Hg <sup>2+</sup>	SWV	GCE	3.4×10 <sup>-3</sup> 1.7×10 <sup>-3</sup>		0.01 – 0.15 0.01 – 0.1	Au NPs, DNA	Natural water, orange juice, wine	105
As <sup>3+</sup>	SWASV	GCE	1.29×10 <sup>-4</sup>	1015	1.33×10 <sup>-3</sup> – 0.27	Au NPs	Natural water	106
Pb <sup>2+</sup>	SWASV	GCE	0.15	10.07	0.5 – 8	Amine	Waste water	107
Pb <sup>2+</sup> Cd <sup>2+</sup>	SWASV	GCE	1.4×10 <sup>-5</sup> 9.2×10 <sup>-5</sup>	235 196	5×10 <sup>-3</sup> – 0.6 0.02 – 0.59	polydopamine	Aqueous effluent	108
Cd <sup>2+</sup>	SWASV	GCE	0.056	14.82	0 – 0.8	Reduced graphene oxide		109
Pb <sup>2+</sup>	SWASV	GCE	0.17 0.073 0.033 0.05 0.04	13.6 7.4 2.4 10.1 4.35	0.4 – 1.5 0.7 – 1.2 0.8 – 1.2 0.5 – 1.5 0.4 – 1.1	Reduced graphene oxide		103
Cu <sup>2+</sup> Cd <sup>2+</sup> Cu <sup>2+</sup>	SWASV	CPE	1.78×10 <sup>-3</sup> 0.014			Macrocyclic Schiff-base ligand	Carrot, fish, rice,	117

<b>Hg<sup>2+</sup></b>			$4.98 \times 10^{-3}$				different waters	
<b>Pb<sup>2+</sup></b>	SWASV	GCE	0.119	14.9	0.3 – 1.3		River water	110
<b>Cd<sup>2+</sup></b>			0.154	3.18	0.3 – 1.3			
<b>Hg<sup>2+</sup></b>			0.0839	7.67	1.3 – 1.8			
<b>Cu<sup>2+</sup></b>			0.0765	4.73	0.3 – 1.7			
<b>Pb<sup>2+</sup></b>	SWASV	GCE	0.0422	50.6	0.1 – 1.3	Chitosan	River water	111
<b>Hg<sup>2+</sup></b>			0.0957	9.65	0.4 – 1.1			
<b>Cu<sup>2+</sup></b>			0.0967	4.24	0.3 – 1.2			
<b>Cd<sup>2+</sup></b>			0.0392	8.11	1.2 – 1.7			
<b>Cd<sup>2+</sup></b>	SWASV	GCE	0.2	12.15	0.4 – 1.1	Terephthalic acid	River water	102
<b>Pb<sup>2+</sup></b>			0.04	8.56	0.4 – 1.1			
<b>Hg<sup>2+</sup></b>			0.3	13.81	0.4 – 1.1			
<b>Cd<sup>2+</sup></b>	SWASV	GCE	$1.52 \times 10^{-3}$	8.4	$4.4 \times 10^{-3} - 0.89$	Glutathione	Natural water	112
<b>Pb<sup>2+</sup></b>			$8.78 \times 10^{-4}$	27.37	$2.41 \times 10^{-3} - 0.48$			
<b>Ni<sup>2+</sup></b>	LSV	Pt	$3.5 \times 10^{-3}$		$5 \times 10^{-2} - 1$	Chitosan	Sewage water, urine	113
					3 – 100			
<b>Cr<sup>6+</sup></b>	LSV	SPCE	0.01		0.5 - 10	Au NPs, Sephadex G-150	Lake water	114
<b>Ag<sup>+</sup></b>	DPV	GCE	0.059		0.117 – 17.7	Au NPs	Lake, tap, synthesized water	115
<b>Cu<sup>2+</sup></b>	DPV	GCE	$0.5 \times 10^{-3}$			Multi-walled carbon nanotubes, poly-3-nitroaniline		116

340 Abbreviations: CPE carbon paste electrode

341

342 Lead and cadmium are the most studied heavy metal ions with Fe<sub>3</sub>O<sub>4</sub> NPs. The lowest LODs and highest  
343 sensitivities for both ions were detected by Song et al. who coated the magnetic nanoparticles with polydopamine.  
344 Additionally, the proposed method that uses SWASV was applied for the determination of lead in aqueous effluents  
345 of a factory. The method proved to be successful and comparable with ICP-AES [108]. Moreover, it is worthy to  
346 note that square wave voltammetry and glassy carbon electrodes are the most commonly used when working with  
347 Fe<sub>3</sub>O<sub>4</sub> NPs.

348 Recent studies have reported that the addition of another metal to iron oxide to produce spinel ferrites can  
349 enhance its electrochemical behavior towards some heavy metals. All the groups relied on a solvothermal method  
350 for the synthesis of MnFe<sub>2</sub>O<sub>4</sub> along with surface modifications when applicable. The ferrite nanoparticles prepared  
351 had a spherical morphology with sizes ranging between 200 and 400 nm.

352 In this regard, one group has done different studies on MnFe<sub>2</sub>O<sub>4</sub> to detect different heavy metals. Zhou et  
353 al. successfully synthesized MnFe<sub>2</sub>O<sub>4</sub> nanocrystals and used them to modify a gold electrode and detect As (III)  
354 using SWASV. A linear response was obtained at As concentrations between 10 and 100 ppb with a limit of  
355 detection of 1.95 ppb and a sensitivity of 0.295 μA/ppb. The sensor was successfully applied in tap water for the  
356 detection of arsenic in tap water with a recovery of 95.6% [118]. In another attempt to detect As (III), they modified  
357 a glassy carbon electrode with MnFe<sub>2</sub>O<sub>4</sub> and gold nanoparticles. Using SWASV, the electrode showed a sensitivity  
358 of 0.315 μA/ppb and a LOD of 3.37 ppb with the sensor also being used to test tap water [119], proving that a similar  
359 sensitivity and lower LOD for the detection of As (III) were obtained without modification with gold nanoparticles.  
360 Then, the same group modified a glassy carbon electrode with these nanoparticles for the selective determination  
361 of Pb<sup>2+</sup>. Using SWASV, a sensitivity of 19.9 μA.μM<sup>-1</sup> and LOD of 0.054 μM were obtained under optimized  
362 conditions, while the response to Cd<sup>2+</sup>, Hg<sup>2+</sup>, Cu<sup>2+</sup> and Zn<sup>2+</sup> was poor. The modified electrode was successfully used  
363 to detect a spiked lead concentration in river water [120].

364 In a later study, and in attempt to obtain a better analytical performance, Zhou et al. also used MnFe<sub>2</sub>O<sub>4</sub>  
365 and graphene oxide to modify a glassy carbon electrode for the detection of Pb (II), Cd (II), Cu (II) and Hg (II). Using  
366 square wave anodic stripping voltammetry, the best electrochemical response was obtained for Pb (II) with a  
367 sensitivity of 33.9 mA/mM and a LOD of 0.0883 mM. The sensitivities for Cd (II), Cu (II) and Hg (II) were 13.5  
368 mA/mM, 13 mA/mM and 5.79 mA/mM, respectively. Moreover, the limits of detection were calculated to be 0.778  
369 mM, 0.0997 mM and 1.16 mM, respectively, with a successful application in the analysis of river water [121]. They  
370 also tried modifying a glassy carbon electrode with L-cysteine functionalized MnFe<sub>2</sub>O<sub>4</sub> to detect Pb (II), Hg (II), Cu  
371 (II) and Cd (II) by SWASV. The developed sensor was particularly selective towards lead, with sensitivities of 57  
372 μA/μM and 35.3 μA/μM and LODs of 0.0843 μM and 0.0607 μM under individual and simultaneous conditions of  
373 detection. The sensor was also successfully used to monitor the concentration of lead in river water [122]. Thus, all  
374 attempts to modify MnFe<sub>2</sub>O<sub>4</sub> nanoparticles to detect different heavy metal ions have showed a higher selectivity and  
375 preference for Pb (II). Moreover, although all studies have checked the practicability of the different modified  
376 sensors in real water samples, more experimentation should be done in this regard by monitoring the ions in water  
377 samples other than tap and river water.

378

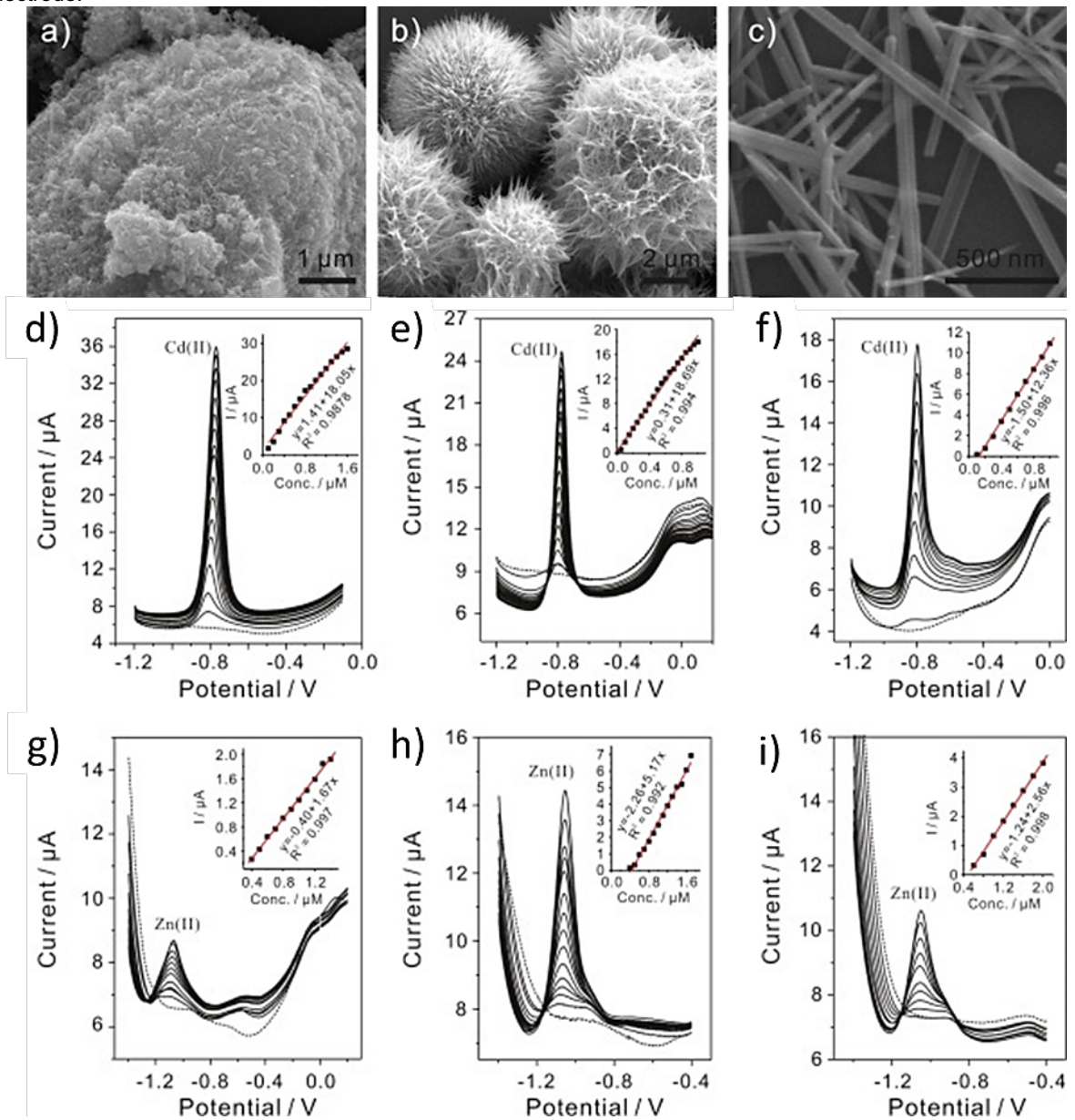
#### 379 4.2. Other metal oxide nanoparticles

380  $\text{Co}_3\text{O}_4$  nanoparticles are one of the most versatile transition metal oxides mainly because of their high  
381 reactivity, superior stability and excellent electrocatalytic activity. Salimi et al. electrodeposited cobalt oxide  
382 nanoparticles on a glassy carbon electrode in order to detect Arsenic (III) using cyclic voltammetry. The  
383 nanoparticles were small in size (100 nm) and uniformly distributed on the surface of the electrode. The results  
384 exhibited a detection limit of 0.6  $\mu\text{M}$  and no interferences in presence of other heavy metal ions with a linear range  
385 of 10 – 50  $\mu\text{M}$ . The possibility to use this sensor for the analysis of water samples was tested on drinking water  
386 from a village in Kurdistan and a concentration of 2.1  $\mu\text{M}$  of As was found in water and confirmed by atomic  
387 absorption spectrometry [123].

388 On the other hand, titanium oxide nanoparticles have attracted attention due to their biocompatibility, high  
389 conductivity, stability and low cost.  $\text{TiO}_2$  nanoparticles were used to detect Hg (II) by Zhou et al. Titanium oxide  
390 nanoparticles were prepared using sol-gel process. Briefly, tetrabutyl titanate was dissolved in ethanol and acetic  
391 acid, after which water was added dropwise with vigorous stirring until a white transparent sol was formed. The sol  
392 was transformed into a gel, dried and calcinated to obtain  $\text{TiO}_2$  powder. The nanoparticles, along with gold  
393 nanoparticles, were used to modify a gold electrode with the help of chitosan as a binder. Characterization showed  
394 that  $\text{TiO}_2$  nanoparticles had a size range between 5 and 15 nm, with gold nanoparticles on their surface. In a medium  
395 buffered at a pH of 5 and using differential pulse anodic stripping voltammetry, the sensor showed a wide linear  
396 concentration range of Hg (II) from 5 to 400 nM and a low detection limit of 1 nM with a sensitivity of 3.133  $\mu\text{A}\cdot\mu\text{M}^{-1}$   
397 and no interference from different ions. Moreover, the sensor was tested for Hg (II) in some water samples, and  
398 the recoveries were between 98 and 106% for all samples [124]. Zhang et al. used purchased titanium oxide  
399 nanoparticle to modify a gold strip electrode to detect As (III) by linear sweep voltammetry. The linear range of  
400 analysis was obtained between 10  $\mu\text{g/L}$  and 80  $\mu\text{g/L}$  with a limit of detection of 10  $\mu\text{g/L}$  and the possibility to use it  
401 for arsenic determination in real samples. Moreover, the stability of the electrodes was investigated and 96% of the  
402 initial response current was retained after 15 days [125]. Mao et al. incorporated  $\text{TiO}_2$  nanoparticles into multiwalled  
403 carbon nanotubes and a cationic surfactant to modify a glassy carbon electrode. LSASV was used for the  
404 determination of mercury (II) and a linear range of 0.1 – 100  $\mu\text{M}$  with a limit of detection of 0.025  $\mu\text{M}$  were obtained.  
405 The potential applicability of the sensor was evaluated in spiked and non-spiked samples of river and industrial  
406 wastewater, and the sensor was able to successfully detect mercury in the wastewater even before spiking [126].  
407 Ramezani et al. constructed an electrochemical sensor using spherical  $\text{TiO}_2$  nanoparticles intermixed with graphite  
408 powder and 1,2-bis-[o-aminophenyl thio] ethane. Using DPASV, and under optimum conditions, Cd (II) was  
409 detected in a linear concentration range of 2.9 nM – 4.6  $\mu\text{M}$  with a limit of detection of 2 nM. A spiked concentration  
410 of Cd (II) ions in tap water was successfully detected without requiring any treatment of the water [127]. Liu et al  
411 used an  $\text{Fe}_3\text{O}_4\text{-TiO}_2$  core-shell nanoparticles on a glassy carbon electrode for the detection of Pb (II). Using square  
412 wave voltammetry (SWV), the limit of detection of the proposed sensor was calculated to be  $7.5\times 10^{-13}$  M with a  
413 linear range of  $4\times 10^{-13}$  M –  $2.5\times 10^{-8}$  M. Different concentrations of Pb (II) were evaluated in river and rain water  
414 samples with recoveries ranging between 99 and 110% [128]. Each one of these modifications with  $\text{TiO}_2$  NPs  
415 presents its advantages, from outstanding limit of detection of  $7.5\times 10^{-13}$  M for Pb (II) [128] to the wide linear range  
416 of detection of 2.9 nM – 4.6  $\mu\text{M}$  for Cd (II) [127]; nevertheless, more experimentation is required in order to be able  
417 to compare between the different methods.

418 Different forms of manganese oxide nanoparticles have been explored due to properties like low cost, non-  
419 toxicity and high activity (mainly in alkali media). Zhang et al. focused on investigating the difference between  
420 various  $\text{MnO}_2$  structures, including nanoparticles, nanotubes and nanobowls on the mutual interference of  $\text{Cd}^{2+}$ ,  
421  $\text{Pb}^{2+}$  and  $\text{Zn}^{2+}$  (figure 7). The nanoparticles were prepared by dissolving potassium permanganate in ethanol,  
422 washing the product with water and drying it. The nanotubes were prepared by dissolving  $\text{MnSO}_4\cdot\text{H}_2\text{O}$  and  $\text{KMnO}_4$   
423 in water, heating the mixture for 12 hours, washing the product with water and drying it. The nanobowls were  
424 hydrothermally prepared by dissolving  $\text{MnSO}_4\cdot\text{H}_2\text{O}$  and  $(\text{NH}_4)_2\text{S}_2\text{O}_8$  in water, heating the mixture for 24 h, washing  
425 the product with water and drying it. The group modified a glassy carbon electrode with  $\text{MnO}_2$  and square wave  
426 anodic stripping voltammetry was applied. The individual response was studied for Cd (II) and Zn (II) and the higher  
427 sensitivities were observed with Cd (II) (18.05  $\mu\text{A}/\mu\text{M}$  for the nanoparticles, 12.36  $\mu\text{A}/\mu\text{M}$  for the nanotubes and  
428 18.69  $\mu\text{A}/\mu\text{M}$  for the nanobowls). However, the interference mechanism was not clearly understood and  
429 demonstrated. Upon fixing the concentration of Zn (II), the trend in the mutual interference between Cd (II) and Zn  
430 (II) was similar on the three morphologies of  $\text{MnO}_2$ . On the other hand, when fixing the Cd (II) concentration, the  
431 interference between Cd (II) and Zn (II) on  $\text{MnO}_2$  nanoparticles was different from that on the other structures.  
432 Similarly, the interference between Cd (II) and Pb (II) on  $\text{MnO}_2$  nanotubes was different from the other morphologies  
433 [129]. Fayazi et al. used  $\text{MnO}_2$  nanotubes for the detection of Hg (II) using differential pulse voltammetry. A simple  
434 chemical precipitation followed by a hydrothermal method were used for the fabrication of halloysite nanotubes –  
435 iron oxide – manganese oxide nanocomposite. The electrode displayed a limit of detection of 0.2  $\mu\text{g}\cdot\text{L}^{-1}$  in a linear  
436 range of 0.5 – 150  $\mu\text{g}\cdot\text{L}^{-1}$ . The proposed sensor was validated for mercury determination in well and aqueduct water  
437 where the concentration of Hg (II) before spiking was below the detection limit and the recoveries after spiking were  
438 close to 100%. [130]. Salimi et al. investigated the use of yet another form of manganese oxide nanoparticles:  
439 nanoflakes. A glassy carbon electrode was first modified with chitosan and multiwalled carbon nanotubes followed  
440 by the electrodeposition of manganese oxide. Using cyclic voltammetry, Cr (III) was detected in a linear range of

441 40 – 360  $\mu\text{M}$ , and the electrode was used for the detection of chromium ions in drinking water samples such that  
 442 the calculated Cr (III) concentration agreed with that measured by AAS [131]. All these studies were nicely  
 443 elaborated, but at the same time each one of them still misses some important data on the analytical performance  
 444 of each electrode.



445  
 446 Figure 7: SEM images of (a) MnO<sub>2</sub> nanoparticles, (b) MnO<sub>2</sub> nanobowls and (c) MnO<sub>2</sub> nanotubes. SWASV responses  
 447 of MnO<sub>2</sub> (d and g) nanoparticles, (e and h) nanobowls and (f and i) nanotubes modified electrode towards Cd (II)  
 448 and Zn (II) at different concentrations in 0.1 M NaAc–HAc (pH 5.0), respectively. The insets are plots of current vs  
 449 concentration of Cd (II) and Zn (II), respectively [129]. Reproduced with permission from Elsevier  
 450

451 Wei et. al used tin oxide nanoparticles with reduced graphene oxide for the determination of Cd<sup>2+</sup>, Pb<sup>2+</sup>,  
 452 Cu<sup>2+</sup> and Hg<sup>2+</sup> by square wave anodic stripping voltammetry. SnO<sub>2</sub> nanoparticles are known to have a high electric  
 453 conductivity and chemical sensitivity, along with the ability to adsorb heavy metal ions. The nanoparticles were  
 454 prepared by a one-step wet chemical method after the preparation of reduced graphene oxide. This step involved  
 455 mixing graphene oxide with SnCl<sub>4</sub>·5H<sub>2</sub>O in water. After stirring and centrifuging, the product was heated to improve  
 456 its crystallinity. The obtained nanoparticles were uniformly distributed on the graphene network, with an average  
 457 diameter of 4 – 5 nm. Individual and simultaneous determination of these ions were done, and the limits of detection  
 458 of the ions were 1.015×10<sup>-10</sup> M, 1.839×10<sup>-10</sup> M, 2.269×10<sup>-10</sup> M and 2.789 ×10<sup>-10</sup> M, respectively, with an enhanced  
 459 sensitivity for Cu (II) and Hg (II) when analyzed simultaneously. The authors reported that even though the  
 460 sensitivities and LODs are not the best, but the electrode can be used without needing regeneration [132]. Yang et  
 461 al. synthesized an amino-based porous SnO<sub>2</sub> nanowires and modified a glassy carbon electrode for the detection  
 462 of Cd (II) by means of SWASV. The sensor displayed a sensitivity of 124.03  $\mu\text{A} \cdot \mu\text{M}^{-1}$  and a limit of detection of

0.0054  $\mu\text{M}$ , with an effective determination of cadmium ions in water samples [133]. Cui and coworkers synthesized a 2-amino benzothiazole and 2-amino-4-thiazoleacetic acid derivative graphene enhanced with fluorine, chlorine and iodine on  $\text{SnO}_2$  nanoparticles for the detection of Cu (II), Cd (II) and Hg (II). The nanoparticles were nearly spherical and well distributed on the graphene sheet. Using cyclic voltammetry, it was shown that the fluorine- $\text{SnO}_2$  sensor is the best suited for the detection of Cu (II), and thus differential pulse voltammetry was used. A linear range from 2 to 1000 nM and a LOD of 0.3 nM were obtained. The electrode was later used for the simultaneous detection of Cd (II), Cu (II) and Hg (II) such that all the linear ranges were between 20 and 2000 nM and the LODs were 5 nM, 3 nM and 5 nM, respectively, and hence the electrode was successfully evaluated for these ions in lake water, with results in agreement with those of AAS [134].

In addition to the general properties of nanoparticles,  $\text{CeO}_2$  has a strong adsorption ability. Li et al. used a glassy carbon electrode modified with cerium oxide ( $\text{CeO}_2$ ) nanoparticles, multi-wall carbon nanotubes, 1-ethyl-3-methylimidazolium tetrafluoroborate ( $\text{EMIMBF}_4$ ) and DNA to detect Pb (II). Differential pulse voltammetry was applied and the linear range for Pb (II) was between  $10^{-8}$  and  $10^{-5}$  M with the detection limit being  $5 \times 10^{-9}$  M hardly exhibiting any interference from five different metal ions with a practical application for the detection of lead in tap water [135].

Yukrid et al. used thermal pyrolysis for the synthesis of ZnO nanorods mixed with graphene solution through colloidal coagulation for the modification of a screen-printed carbon electrode. Anodic stripping voltammetry was used for the concurrent determination of  $\text{Cd}^{2+}$  and  $\text{Pb}^{2+}$ . The limits of detection obtained were  $0.6 \mu\text{g.L}^{-1}$  for Cd (II) and  $0.8 \mu\text{g.L}^{-1}$  for Pb (II) in a linear range of 10 – 200  $\mu\text{g.L}^{-1}$ , respectively. These heavy metal ions were simultaneously determined in wastewater samples, with measurements in accordance with those obtained by ICP-OES [136]. Yuan-Yuan et al. prepared a ZnO nanotubes/reduced graphene modified glassy carbon electrode via electrospinning and thermal decomposition of zinc acetate-polyacrylonitrile-polyvinyl pyrrolidone. SWASV was used for the analysis of Pb (II). A linear concentration range of  $2.4 \times 10^{-9}$ –  $4.8 \times 10^{-7}$  M and the limit of detection was  $4.8 \times 10^{-10}$  M [137].

MgO nanoflowers were also used for the detection of Pb (II) and Cd (II). Their synthesis involved mixing a magnesium precursor with potassium carbonate and heating the mixture to obtain a white precipitate that was later collected and calcinated. These nanoflowers along with Nafion® were used to modify a glassy carbon macroelectrode and SWASV was used under optimized conditions. The results for Pb (II) and Cd (II) detection showed linear ranges between 1 and 30 nM for lead and between 20 and 140 nM for cadmium, sensitivities of 0.706 and  $0.077 \mu\text{A.nM}^{-1}$  and limits of detection of  $2.1 \times 10^{-12}$  M and  $8.1 \times 10^{-11}$  M, respectively. The sensor was successfully tested for Pb (II) in Reservoir water samples from China [138].

## 5. Summary and Perspectives

Electrochemical methods have been extensively used for the detection of heavy metals. However, the use of metal and metal oxide nanoparticles for modifying electrochemical sensors, for the voltammetric detection of heavy metals, proves to be more promising. Taking advantage of the unique properties of nanoparticles along with the advantages of electrochemical detection over conventional detection techniques, the analytical performance of all the reported electrodes was enhanced. The result was a rapid response time, increased sensitivity, very low limits of detection, simplified operational procedures and enhanced reproducibility.

In this review, the emphasis was on electrochemical sensors that could be applied for water samples. However, different water systems exist, from sea water, river water, tap water, drinking water to wastewater. Thus, these matrices are considered complex, some more than others, with the presence of different heavy metals either free or complexed, cations and anions, organic and inorganic materials... Despite the claims that some of the fabricated sensors were tested in these complex matrices, transition to commercialization remains shy. Moreover, most of these sensors require significant improvements, especially in the selectivity and capability of simultaneous analysis, before they can be applied for commercial use. Besides, commercialization also presents the challenges of reusability and mass production, which question the simplicity and cost-effectiveness of some of the sensors. For example, great focus has been given to gold nanoparticles and some excellent electrochemical sensors have been developed for the detection of heavy metals with LODs much lower than those obtained with  $\text{Fe}_3\text{O}_4$  NPs for instance. Nonetheless, noble metals such as gold and silver are known to be costly, and hence an alternative that presents high selectivity and can detect limits lower than the guidelines such as  $\text{Fe}_3\text{O}_4$  NPs would be convenient. On the other hand, several materials were used along with the nanoparticles for the modification of the electrodes. However, with the use of all these nanoparticles, a few inconveniences, including toxicity and non-biocompatibility during the synthesis of the modified electrodes, still exist.

Recently, bimetallic nanoparticles are emerging as promising candidates that can overcome the challenges faced by mono-metallic nanoparticles. These materials are the result of combining two different metals, thus offering the advantages of each metal alone, along with new characteristics that arise from blending the two metals. Hence, we expect to see in the near future a major increase in research using bimetallic nanoparticles dedicated for the electrochemical detection of heavy metal ions.

## Acknowledgements



524 The authors acknowledge the financial support of the EU H2020 research and innovation program entitled  
525 KardiaTool grant #768686.

526

527 **Declaration of interests:**

528

529 The authors declare that they have no known competing financial interests or personal relationships that could  
530 have appeared to influence the work reported in this paper.

531

532

533 **\*References:**

534

535 [1] Tchounwou, P. B., Yedjou, C. G., Patlolla, A. K., & Sutton, D. J. (2012). Heavy metal toxicity and the environment.  
536 *Exp Suppl*, 101, 133-164. [https://doi:10.1007/978-3-7643-8340-4\\_6](https://doi:10.1007/978-3-7643-8340-4_6)

537 [2] Barton, J., García, M. B. G., Santos, D. H., Fanjul-Bolado, P., Ribotti, A., McCaul, M., ... & Magni, P. (2016).  
538 Screen-printed electrodes for environmental monitoring of heavy metal ions: a review. *Microchimica Acta*, 183(2),  
539 503-517. <https://doi:10.1007/s00604-015-1651-0>

540 [3] Ariño, C., Serrano, N., Díaz-Cruz, J. M., & Esteban, M. (2017). Voltammetric determination of metal ions beyond  
541 mercury electrodes. A review. *Analytica chimica acta*, 990, 11-53. <https://doi:10.1016/j.aca.2017.07.069>

542 [4] Kumar, P., Kim, K. H., Bansal, V., Lazarides, T., & Kumar, N. (2017). Progress in the sensing techniques for  
543 heavy metal ions using nanomaterials. *Journal of industrial and engineering chemistry*, 54, 30-43.  
544 <https://doi:10.1016/j.jiec.2017.06.010>

545 [5] Sabine Martin, W. G. (2009). Human Health Effects of Heavy Metals. *Environmental Science and Technology*  
546 *Briefs for Citizens*.

547 [6] Turdean, G. L. (2011). Design and Development of Biosensors for the Detection of Heavy Metal Toxicity. *Int. J.*  
548 *Electrochem.*, 2011, 1-15. <https://doi:10.4061/2011/343125>

549 [7] Verma, N., & Singh, M. (2005). Biosensors for heavy metals. *BioMetals*, 18(2), 121-129.  
550 <https://doi:10.1007/s10534-004-5787-3>

551 [8] WHO. *Guidelines for Drinking-water Quality* (4<sup>th</sup> ed.). 2011

552 [9] Corr, J. J., & Larsen, E. H. (1996). Arsenic speciation by liquid chromatography coupled with ionspray tandem  
553 mass spectrometry. *J. Anal. At. Spectrom.*, 11(12), 1215. <https://doi:10.1039/ja9961101215>

554 [10] Yin, C., Iqbal, J., Hu, H., Liu, B., Zhang, L., Zhu, B., & Du, Y. (2012). Sensitive determination of trace mercury  
555 by UV-visible diffuse reflectance spectroscopy after complexation and membrane filtration-enrichment. *J. Hazard.*  
556  *Mater.*, 233-234, 207-212. <https://doi:10.1016/j.jhazmat.2012.07.016>

557 [11] Pohl, P. (2009). Determination of metal content in honey by atomic absorption and emission spectrometries.  
558 *TrAC Trends Anal. Chem.*, 28(1), 117-128. <https://doi:10.1016/j.trac.2008.09.015>

559 [12] Gomez-Ariza, J. L., Lorenzo, F., & Garcia-Barrera, T. (2005). Comparative study of atomic fluorescence  
560 spectroscopy and inductively coupled plasma mass spectrometry for mercury and arsenic multispeciation. *Anal.*  
561 *Bioanal. Chem.*, 382(2), 485-492. <https://doi:10.1007/s00216-005-3094-7>

562 [13] Aranda, P. R., Pacheco, P. H., Olsina, R. A., Martinez, L. D., & Gil, R. A. (2009). Total and inorganic mercury  
563 determination in biodiesel by emulsion sample introduction and FI-CV-AFS after multivariate optimization. *J. Anal.*  
564 *At. Spectrom.*, 24(10). <https://doi:10.1039/b903113h>

565 [14] Chen, S.-H., Li, Y.-X., Li, P.-H., Xiao, X.-Y., Jiang, M., Li, S.-S., Liu, W.-Q. (2018). Electrochemical spectral  
566 methods for trace detection of heavy metals: A review. *TrAC Trends Anal. Chem*, 106, 139-150.  
567 <https://doi:10.1016/j.trac.2018.07.005>

568 [15] Lu, Y., Liang, X., Niyungeko, C., Zhou, J., Xu, J., & Tian, G. (2018). A review of the identification and detection  
569 of heavy metal ions in the environment by voltammetry. *Talanta*, 178, 324-338.  
570 <https://doi:10.1016/j.talanta.2017.08.033>

571 [16] Aragay, G., & Merkoçi, A. (2012). Nanomaterials application in electrochemical detection of heavy metals.  
572 *Electrochim. Acta*, 84, 49-61. <https://doi:10.1016/j.electacta.2012.04.044>

- 573 [17] Bansod, B., Kumar, T., Thakur, R., Rana, S., & Singh, I. (2017). A review on various electrochemical techniques  
574 for heavy metal ions detection with different sensing platforms. *Biosens. Bioelectron.*, 94, 443-455.  
575 <https://doi:10.1016/j.bios.2017.03.031>
- 576 [18] Lu, Y., Liang, X., Niyungeko, C., Zhou, J., Xu, J., & Tian, G. (2018). A review of the identification and detection  
577 of heavy metal ions in the environment by voltammetry. *Talanta*, 178, 324-338.  
578 <https://doi:10.1016/j.talanta.2017.08.033>
- 579 [19] Hoyos-Arbeláez, J., Vázquez, M., & Contreras-Calderón, J. (2017). Electrochemical methods as a tool for  
580 determining the antioxidant capacity of food and beverages: A review. *Food Chemistry*, 221, 1371-1381.  
581 <https://doi:10.1016/j.foodchem.2016.11.017>
- 582 [20] Borrill, A., Reily, N. E., & Macpherson, J. V. (2019). Addressing the Practicalities of Anodic Stripping  
583 Voltammetry for Heavy Metal Detection: A Tutorial Review. *The Analyst*. <https://doi:10.1039/c9an01437c>
- 584 [21] Berek, J., Fogg, A. G., Muck, A., & Zima, J. (2001). Polarography and Voltammetry at Mercury Electrodes.  
585 *Critical Reviews in Analytical Chemistry*, 31(4), 291-309. <https://doi:10.1080/20014091076776>
- 586 [22] Cheng, Y., Li, H., Fang, C., Ai, L., Chen, J., Su, J., Fu, Q. (2019). Facile synthesis of reduced graphene  
587 oxide/silver nanoparticles composites and their application for detecting heavy metal ions. *J. Alloys Compd.*, 787,  
588 683-693. <http://doi:10.1016/j.jallcom.2019.01.320>
- 589 [23] Han, T., Jin, J., Wang, C., Sun, Y., Zhang, Y., & Liu, Y. (2017). Ag Nanoparticles-Modified 3D Graphene Foam  
590 for Binder-Free Electrodes of Electrochemical Sensors. *Nanomaterials (Basel)*, 7(2).  
591 <https://doi:10.3390/nano7020040>
- 592 [24] Xing, S., Xu, H., Chen, J., Shi, G., & Jin, L. (2011). Nafion stabilized silver nanoparticles modified electrode  
593 and its application to Cr(VI) detection. *J. Electroanal. Chem.*, 652(1-2), 60-65.  
594 <https://doi:10.1016/j.jelechem.2010.03.035>
- 595 [25] Renedo, O. D., & Julia Arcos Martínez, M. (2007). A novel method for the anodic stripping voltammetry  
596 determination of Sb(III) using silver nanoparticle-modified screen-printed electrodes. *Electrochem. Commun.*, 9(4),  
597 820-826. <https://doi:10.1016/j.elecom.2006.11.016>
- 598 [26] Zeng, S., Yong, K.-T., Roy, I., Dinh, X.-Q., Yu, X., & Luan, F. (2011). A Review on Functionalized Gold  
599 Nanoparticles for Biosensing Applications. *Plasmonics*, 6(3), 491-506. <https://doi:10.1007/s11468-011-9228-1>
- 600 [27] Hassan, S. S., Sirajuddin, Solangi, A. R., Kazi, T. G., Kalhor, M. S., Junejo, Y., Kalwar, N. H. (2012). Nafion  
601 stabilized ibuprofen-gold nanostructures modified screen printed electrode as arsenic(III) sensor. *J. Electroanal.*  
602 *Chem.*, 682, 77-82. <https://doi:10.1016/j.jelechem.2012.07.006>
- 603 [28] Ouyang, R., Bragg, S. A., Chambers, J. Q., & Xue, Z. L. (2012). Flower-like self-assembly of gold nanoparticles  
604 for highly sensitive electrochemical detection of chromium(VI). *Anal. Chim. Acta*, 722, 1-7.  
605 <https://doi:10.1016/j.aca.2012.01.032>
- 606 [29] Dutta, S., Strack, G., & Kurup, P. (2018). Gold Nanostar Electrodes for Heavy Metal Detection. *Sensors and*  
607 *Actuators B: Chemical*. <https://doi:10.1016/j.snb.2018.10.111>
- 608 [30] Dutta, S., Strack, G., & Kurup, P. (2019). Gold nanostar-based voltammetric sensor for chromium(VI).  
609 *Microchim. Acta*, 186(11). <https://doi:10.1007/s00604-019-3847-1>
- 610 [31] Lu, D., Sullivan, C., Brack, E. M., Drew, C. P., & Kurup, P. (2020). Simultaneous voltammetric detection of  
611 cadmium(II), arsenic(III), and selenium(IV) using gold nanostar-modified screen-printed carbon electrodes and  
612 modified Britton-Robinson buffer. *Analytical and Bioanalytical Chemistry*. <https://doi:10.1007/s00216-020-02642-4>
- 613 [32] Yang, X., Xu, J., Tang, X., Liu, H., & Tian, D. (2010). A novel electrochemical DNAzyme sensor for the  
614 amplified detection of Pb<sup>2+</sup> ions. *Chem. Commun. (Camb)*, 46(18), 3107-3109. <https://doi:10.1039/c002137g>
- 615 [33] Pooi See, W., Nathan, S., & Yook Heng, L. (2011). A Disposable Copper (II) Ion Biosensor Based on Self-  
616 Assembly of L-Cysteine on Gold Nanoparticle-Modified Screen-Printed Carbon Electrode. *Journal of Sensors*,  
617 2011, 1-5. <https://doi:10.1155/2011/230535>
- 618 [34] Safavi, A., & Farjami, E. (2011). Construction of a carbon nanocomposite electrode based on amino acids  
619 functionalized gold nanoparticles for trace electrochemical detection of mercury. *Anal. Chim. Acta*, 688(1), 43-48.  
620 <https://doi:10.1016/j.aca.2010.12.001>

- 621 [35] Zhu, L., Xu, L., Huang, B., Jia, N., Tan, L., & Yao, S. (2014). Simultaneous determination of Cd(II) and Pb(II)  
622 using square wave anodic stripping voltammetry at a gold nanoparticle-graphene-cysteine composite modified  
623 bismuth film electrode. *Electrochim. Acta*, 115, 471-477. <https://doi:10.1016/j.electacta.2013.10.209>
- 624 [36] Xu, G., Wang, G., He, X., Zhu, Y., Chen, L., & Zhang, X. (2013). An ultrasensitive electrochemical method for  
625 detection of Ag(+) based on cyclic amplification of exonuclease III activity on cytosine-Ag(+)-cytosine. *Analyst*,  
626 138(22), 6900-6906. <https://doi:10.1039/c3an01320k>
- 627 [37] Chen, Z., Li, L., Mu, X., Zhao, H., & Guo, L. (2011). Electrochemical aptasensor for detection of copper based  
628 on a reagentless signal-on architecture and amplification by gold nanoparticles. *Talanta*, 85(1), 730-735.  
629 <https://doi:10.1016/j.talanta.2011.04.056>
- 630 [38] Kong, R. M., Zhang, X. B., Zhang, L. L., Jin, X. Y., Huan, S. Y., Shen, G. L., & Yu, R. Q. (2009). An ultrasensitive  
631 electrochemical "turn-on" label-free biosensor for Hg<sup>2+</sup> with AuNP-functionalized reporter DNA as a signal amplifier.  
632 *Chem. Commun. (Camb)*(37), 5633-5635. <https://doi:10.1039/b911163h>
- 633 [39] Lu, X., Dong, X., Zhang, K., & Zhang, Y. (2012). An ultrasensitive electrochemical mercury(II) ion biosensor  
634 based on a glassy carbon electrode modified with multi-walled carbon nanotubes and gold nanoparticles. *Analytical*  
635 *Methods*, 4(10). <https://doi:10.1039/c2ay25634g>
- 636 [40] Tang, X., Liu, H., Zou, B., Tian, D., & Huang, H. (2012). A fishnet electrochemical Hg<sup>2+</sup> sensing strategy based  
637 on gold nanoparticle-bioconjugate and thymine-Hg(2+)-thymine coordination chemistry. *Analyst*, 137(2), 309-311.  
638 <https://doi:10.1039/c1an15908a>
- 639 [41] Xuan Dai, O. N., Michael E. Hyde, and Richard G. Compton. (2004). Anodic Stripping Voltammetry of  
640 Arsenic(III) Using Gold Nanoparticle-Modified Electrodes. *Anal. Chem.*, 76, 5924-5929.  
641 <https://doi:10.1021/ac049232x>
- 642 [42] Xiao, L., Wildgoose, G. G., & Compton, R. G. (2008). Sensitive electrochemical detection of arsenic (III) using  
643 gold nanoparticle modified carbon nanotubes via anodic stripping voltammetry. *Anal. Chim. Acta*, 620(1-2), 44-49.  
644 <https://doi:10.1016/j.aca.2008.05.015>
- 645 [43] Carrera, P., Espinoza-Montero, P. J., Fernández, L., Romero, H., & Alvarado, J. (2017). Electrochemical  
646 determination of arsenic in natural waters using carbon fiber ultra-microelectrodes modified with gold nanoparticles.  
647 *Talanta*, 166, 198–206. <https://doi:10.1016/j.talanta.2017.01.056>
- 648 [44] Raj, B. K. J. a. C. R. (2008). Gold Nanoelectrode Ensembles for the Simultaneous Electrochemical Detection  
649 of Ultratrace Arsenic, Mercury, and Copper. *Anal. Chem.*, 80, 4836–4844.
- 650 [45] Zhao, G., & Liu, G. (2018). Electrochemical Deposition of Gold Nanoparticles on Reduced Graphene Oxide by  
651 Fast Scan Cyclic Voltammetry for the Sensitive Determination of As(III). *Nanomaterials*, 9(1), 41.  
652 <https://doi:10.3390/nano9010041>
- 653 [46] Ehsan Majid, S. H., Yali Liu, Keith B. Male, and John H. T. Luong. (2006). Electrochemical Determination of  
654 Arsenite Using a Gold Nanoparticle Modified Glassy Carbon Electrode and Flow Analysis. *Anal. Chem*, 78, 762-  
655 769. <https://doi:10.1021/ac0513562>
- 656 [47] Hossain, M. M., Islam, M. M., Ferdousi, S., Okajima, T., & Ohsaka, T. (2008). Anodic Stripping Voltammetric  
657 Detection of Arsenic(III) at Gold Nanoparticle-Modified Glassy Carbon Electrodes Prepared by Electrodeposition in  
658 the Presence of Various Additives. *Electroanalysis*, 20(22), 2435-2441. <https://doi:10.1002/elan.200804339>
- 659 [48] Buffa, A., & Mandler, D. (2019). Arsenic(III) detection in water by flow-through carbon nanotube membrane  
660 decorated by gold nanoparticles. *Electrochimica Acta*. <https://doi:10.1016/j.electacta.2019.06.114>
- 661 [49] Bu, L., Liu, J., Xie, Q., & Yao, S. (2015). Anodic stripping voltammetric analysis of trace arsenic(III) enhanced  
662 by mild hydrogen-evolution at a bimetallic Au–Pt nanoparticle modified glassy carbon electrode. *Electrochemistry*  
663 *Communications*, 59, 28–31. <https://doi:10.1016/j.elecom.2015.06.015>
- 664 [50] Bu, L., Xie, Q., & Ming, H. (2020). Gold nanoparticles decorated three-dimensional porous graphitic carbon  
665 nitrides for sensitive anodic stripping voltammetric analysis of trace arsenic(III). *Journal of Alloys and Compounds*,  
666 153723. <https://doi:10.1016/j.jallcom.2020.153723>
- 667 [51] Muniyandi Rajkumar, S. T., Shen-Ming Chen. (2011). Electrochemical Detection of Arsenic in Various Water  
668 Samples. *Int. J. Electrochem. Sci.*, 6, 3164 - 3177.
- 669 [52] Song, Y.-S., Muthuraman, G., Chen, Y.-Z., Lin, C.-C., & Zen, J.-M. (2006). Screen Printed Carbon Electrode  
670 Modified with Poly(L-Lactide) Stabilized Gold Nanoparticles for Sensitive As(III) Detection. *Electroanalysis*, 18(18),  
671 1763-1770. <https://doi:10.1002/elan.200603634>
- 672 [53] Baron, R., Šljukić, B., Salter, C., Crossley, A., & Compton, R. G. (2007). Electrochemical detection of arsenic  
673 on a gold nanoparticle array. *Russ. J. Phys. Chem. A*, 81(9), 1443-1447. <https://doi:10.1134/s003602440709018x>

- 674 [54] Lei Zhang, Da-Wei Li, Wei Song, Lei Shi, Yang Li, & Yi-Tao Long. (2010). High Sensitive On-Site Cadmium  
675 Sensor Based on AuNPs Amalgam Modified Screen-Printed Carbon Electrodes. *IEEE Sensors Journal*, 10(10),  
676 1583–1588. <https://doi:10.1109/jsen.2010.2046408>
- 677 [55] Si, Y., Liu, J., Chen, Y., Miao, X., Ye, F., Liu, Z., & Li, J. (2018). rGO/AuNPs/tetraphenylporphyrin  
678 nanoconjugate-based electrochemical sensor for highly sensitive detection of cadmium ions. *Analytical Methods*,  
679 10(29), 3631-3636. <https://doi:10.1039/c8ay01020j>
- 680 [56] Xu, X., Duan, G., Li, Y., Liu, G., Wang, J., Zhang, H., Cai, W. (2014). Fabrication of gold nanoparticles by laser  
681 ablation in liquid and their application for simultaneous electrochemical detection of Cd<sup>2+</sup>, Pb<sup>2+</sup>, Cu<sup>2+</sup>, Hg<sup>2+</sup>. *ACS*  
682 *Appl. Mater. Interfaces*, 6(1), 65-71. <https://doi:10.1021/am404816e>
- 683 [57] Zhang, B., Chen, J., Zhu, H., Yang, T., Zou, M., Zhang, M., & Du, M. (2016). Facile and green fabrication of  
684 size-controlled AuNPs/CNFs hybrids for the highly sensitive simultaneous detection of heavy metal ions.  
685 *Electrochim. Acta*, 196, 422-430. <https://doi:10.1016/j.electacta.2016.02.163>
- 686 [58] Priya, T., Dhanalakshmi, N., Thennarasu, S., Karthikeyan, V., & Thinakaran, N. (2019). Ultra sensitive  
687 electrochemical detection of Cd<sup>2+</sup> and Pb<sup>2+</sup> using penetrable nature of graphene/gold nanoparticles/modified L-  
688 cysteine nanocomposite. *Chemical Physics Letters*, 731, 136621. <https://doi:10.1016/j.cplett.2019.136621>
- 689 [59] Welch, C. M., Nekrassova, O., Dai, X., Hyde, M. E., & Compton, R. G. (2004). Fabrication, characterisation  
690 and voltammetric studies of gold amalgam nanoparticle modified electrodes. *ChemPhysChem*, 5(9), 1405-1410.  
691 <https://doi:10.1002/cphc.200400263>
- 692 [60] Guodong Liu, Y.-Y. L., Hong Wu, and Yuehe Lin. (2007). Voltammetric Detection of Cr(VI) with Disposable  
693 Screen-Printed Electrode Modified with Gold Nanoparticles. *Environ. Sci. Technol.*, 41, 8129–8134.  
694 <https://doi:10.1021/es071726z>
- 695 [61] Benzhi Liu, L. L., Min Wang and Yanqin Zi. (2008). A study of nanostructured gold modified glassy carbon  
696 electrode for the determination of trace Cr(VI). *J. Chem. Sci.*, 120(5), 493–498. <https://doi:10.1007/s12039-008-0077-1>
- 698 [62] Wang, N., Lin, M., Dai, H., & Ma, H. (2016). Functionalized gold nanoparticles/reduced graphene oxide  
699 nanocomposites for ultrasensitive electrochemical sensing of mercury ions based on thymine-mercury-thymine  
700 structure. *Biosens. Bioelectron.*, 79, 320-326. <https://doi:10.1016/j.bios.2015.12.056>
- 701 [63] Zhou, N., Chen, H., Li, J., & Chen, L. (2013). Highly sensitive and selective voltammetric detection of mercury(II)  
702 using an ITO electrode modified with 5-methyl-2-thiouracil, graphene oxide and gold nanoparticles. *Microchim.*  
703 *Acta*, 180(5-6), 493-499. <https://doi:10.1007/s00604-013-0956-0>
- 704 [64] Li Shen, Z. C., Yihan Li, Shali He, Shubao Xie, Xiaodong Xu, Zhongwei Liang, Xin Meng, Qing Li, Zhiwei Zhu,  
705 Meixian Li, X. Chris Le, and Yuanhua Shao. (2008). Electrochemical DNAzyme Sensor for Lead Based on  
706 Amplification of DNA-Au Bio-Bar Codes. *Anal. Chem.*, 80, 6323–6328. <https://doi:10.1021/ac800601>
- 707 [65] Fu, X. C., Wu, J., Nie, L., Xie, C. G., Liu, J. H., & Huang, X. J. (2012). Electropolymerized surface ion imprinting  
708 films on a gold nanoparticles/single-wall carbon nanotube nanohybrids modified glassy carbon electrode for  
709 electrochemical detection of trace mercury(II) in water. *Anal. Chim. Acta*, 720, 29-37.  
710 <https://doi:10.1016/j.aca.2011.12.071>
- 711 [66] Lin, Y., Peng, Y., & Di, J. (2015). Electrochemical detection of Hg(II) ions based on nanoporous gold  
712 nanoparticles modified indium tin oxide electrode. *Sens. Actuators, B* 220, 1086-1090.  
713 <https://doi:10.1016/j.snb.2015.06.064>
- 714 [67] O. Abollino; A. Giacomino; M. Malandrino; G. Piscionieri; E. Mentasti. (2007), Determination of mercury by  
715 anodic stripping voltammetry at a gold nanoparticle-modified glassy carbon electrode pp. 182-182.  
716 <https://doi:10.1002/elan.200704044>
- 717 [68] Ting, S. L., Ee, S. J., Ananthanarayanan, A., Leong, K. C., & Chen, P. (2015). Graphene quantum dots  
718 functionalized gold nanoparticles for sensitive electrochemical detection of heavy metal ions. *Electrochim. Acta*,  
719 172, 7-11. <https://doi:10.1016/j.electacta.2015.01.026>
- 720 [69] Miao, P., Liu, L., Li, Y., & Li, G. (2009). A novel electrochemical method to detect mercury (II) ions. *Electrochem.*  
721 *Commun.*, 11(10), 1904-1907. <https://doi:10.1016/j.elecom.2009.08.013>
- 722 [70] Wan, H., Sun, Q., Li, H., Sun, F., Hu, N., & Wang, P. (2015). Screen-printed gold electrode with gold  
723 nanoparticles modification for simultaneous electrochemical determination of lead and copper. *Sens. Actuators, B*,  
724 209, 336-342. <https://doi:10.1016/j.snb.2014.11.127>
- 725 [71] Martín-Yerga, D., González-García, M. B., & Costa-García, A. (2012). Use of nanohybrid materials as  
726 electrochemical transducers for mercury sensors. *Sens. Actuators, B* 165(1), 143-150.  
727 <https://doi:10.1016/j.snb.2012.02.031>

- 728 [72] Zhu, L., Xu, L., Huang, B., Jia, N., Tan, L., & Yao, S. (2014). Simultaneous determination of Cd(II) and Pb(II)  
729 using square wave anodic stripping voltammetry at a gold nanoparticle-graphene-cysteine composite modified  
730 bismuth film electrode. *Electrochim. Acta*, 115, 471-477. <https://doi:10.1016/j.electacta.2013.10.209>
- 731 [73] Yiwei, X., Wen, Z., Xiaowei, H., Jiyong, S., Xiaobo, Z., Zhihua, L., & Xueping, C. (2019). Adsorptive stripping  
732 voltammetry determination of hexavalent chromium by a pyridine functionalized gold nanoparticles/three-  
733 dimensional graphene electrode. *Microchemical Journal*, 104022. <https://doi:10.1016/j.microc.2019.104022>
- 734 [74] Dominguez-Renedo, O., Ruiz-Espelt, L., Garcia-Astorgano, N., & Arcos-Martinez, M. J. (2008). Electrochemical  
735 determination of chromium(VI) using metallic nanoparticle-modified carbon screen-printed electrodes. *Talanta*,  
736 76(4), 854-858. <https://doi:10.1016/j.talanta.2008.04.036>
- 737 [75] Tsai, M. C., & Chen, P. Y. (2008). Voltammetric study and electrochemical detection of hexavalent chromium  
738 at gold nanoparticle-electrodeposited indium tin oxide (ITO) electrodes in acidic media. *Talanta*, 76(3), 533-539.  
739 <https://doi:10.1016/j.talanta.2008.03.043>
- 740 [76] Tu, J., Gan, Y., Liang, T., Wan, H., & Wang, P. (2018). A miniaturized electrochemical system for high sensitive  
741 determination of chromium(VI) by screen-printed carbon electrode with gold nanoparticles modification. *Sens.*  
742 *Actuators, B*, 272, 582-588. <https://doi:10.1016/j.snb.2018.06.006>
- 743 [77] Gong, J., Zhou, T., Song, D., & Zhang, L. (2010). Monodispersed Au nanoparticles decorated graphene as an  
744 enhanced sensing platform for ultrasensitive stripping voltammetric detection of mercury(II). *Sensors and Actuators*  
745 *B: Chemical*, 150(2), 491-497. <https://doi:10.1016/j.snb.2010.09.014>
- 746 [78] Bernalte, E., Marín Sánchez, C., & Pinilla Gil, E. (2012). Gold nanoparticles-modified screen-printed carbon  
747 electrodes for anodic stripping voltammetric determination of mercury in ambient water samples. *Sens. Actuators,*  
748 *B*, 161(1), 669-674. <https://doi:10.1016/j.snb.2011.10.088>
- 749 [79] Hezard, T., Fajerweg, K., Evrard, D., Collière, V., Behra, P., & Gros, P. (2012). Gold nanoparticles  
750 electrodeposited on glassy carbon using cyclic voltammetry: Application to Hg(II) trace analysis. *J. Electroanal.*  
751 *Chem.*, 664, 46-52. <https://doi:10.1016/j.jelechem.2011.10.014>
- 752 [80] Akbari Hasanjani, H. R., & Zarei, K. (2019). An electrochemical sensor for attomolar determination of  
753 mercury(II) using DNA/poly-L-methionine-gold nanoparticles/pencil graphite electrode. *Biosens. Bioelectron.*, 128,  
754 1-8. <https://doi:10.1016/j.bios.2018.12.039>
- 755 [81] Zhu, Z., Su, Y., Li, J., Li, D., Zhang, J., Song, S., Fan, C. (2009). Highly sensitive electrochemical sensor for  
756 mercury(II) ions by using a mercury-specific oligonucleotide probe and gold nanoparticle-based amplification. *Anal.*  
757 *Chem.*, 81(18), 7660-7666. <https://doi:10.1021/ac9010809>
- 758 [82] Xu, H., Zeng, L., Xing, S., Shi, G., Xian, Y., & Jin, L. (2008). Microwave-radiated synthesis of gold  
759 nanoparticles/carbon nanotubes composites and its application to voltammetric detection of trace mercury(II).  
760 *Electrochem. Commun.*, 10(12), 1839-1843. <https://doi:10.1016/j.elecom.2008.09.030>
- 761 [83] Lee, P. M., Wang, Z., Liu, X., Chen, Z., & Liu, E. (2015). Glassy carbon electrode modified by graphene-gold  
762 nanocomposite coating for detection of trace lead ions in acetate buffer solution. *Thin Solid Films*, 584, 85-89.  
763 <https://doi:10.1016/j.tsf.2015.03.017>
- 764 [84] Lu, Z., Yang, S., Yang, Q., Luo, S., Liu, C., & Tang, Y. (2013). A glassy carbon electrode modified with  
765 graphene, gold nanoparticles and chitosan for ultrasensitive determination of lead(II). *Microchim. Acta*, 180(7-8),  
766 555-562. <https://doi:10.1007/s00604-013-0959-x>
- 767 [85] Zhu, Y., Zeng, G. M., Zhang, Y., Tang, L., Chen, J., Cheng, M., Zhang, L.H., He, L., Guo, Y., He, X.X., Lai,  
768 M.Y. & He, Y. B. (2014). Highly sensitive electrochemical sensor using a MWCNTs/GNPs-modified electrode for  
769 lead (II) detection based on Pb(2+)-induced G-rich DNA conformation. *Analyst*, 139(19), 5014-5020.  
770 <https://doi:10.1039/c4an00874>
- 771 [86] Dominguez Renedo, O., & Arcos Martinez, M. J. (2007). Anodic stripping voltammetry of antimony using gold  
772 nanoparticle-modified carbon screen-printed electrodes. *Anal. Chim. Acta*, 589(2), 255-260.  
773 <https://doi:10.1016/j.aca.2007.02.069>
- 774 [87] Lee, G.-J., Kim, C. K., Lee, M. K., & Rhee, C. K. (2010). Simultaneous Voltammetric Determination of Zn, Cd  
775 and Pb at Bismuth Nanopowder Electrodes with Various Particle Size Distributions. *Electroanalysis*, 22(5), 530-  
776 535. <https://doi:10.1002/elan.200900356>
- 777 [88] Lee, G.-J., Lee, H. M., Uhm, Y. R., Lee, M. K., & Rhee, C.-K. (2008). Square-wave voltammetric determination  
778 of thallium using surface modified thick-film graphite electrode with Bi nanopowder. *Electrochem. Commun.*, 10(12),  
779 1920-1923. <https://doi:10.1016/j.elecom.2008.10.01>

- 780 [89] Rico, M. A., Olivares-Marin, M., & Gil, E. P. (2009). Modification of carbon screen-printed electrodes by  
781 adsorption of chemically synthesized Bi nanoparticles for the voltammetric stripping detection of Zn(II), Cd(II) and  
782 Pb(II). *Talanta*, 80(2), 631-635. <https://doi:10.1016/j.talanta.2009.07.039>
- 783 [90] Saturno, J., Valera, D., Carrero, H., & Fernández, L. (2011). Electroanalytical detection of Pb, Cd and traces  
784 of Cr at micro/nano-structured bismuth film electrodes. *Sens. Actuators, B*, 159(1), 92-96.  
785 <https://doi:10.1016/j.snb.2011.06.055>
- 786 [91] Sahoo, P. K., Panigrahy, B., Sahoo, S., Satpati, A. K., Li, D., & Bahadur, D. (2013). In situ synthesis and  
787 properties of reduced graphene oxide/Bi nanocomposites: as an electroactive material for analysis of heavy metals.  
788 *Biosens. Bioelectron.*, 43, 293-296. <https://doi:10.1016/j.bios.2012.12.031>
- 789 [92] Campbell, F. W., & Compton, R. G. (2009). The use of nanoparticles in electroanalysis: an updated review.  
790 *Analytical and Bioanalytical Chemistry*, 396(1), 241–259. <https://doi:10.1007/s00216-009-3063-7>
- 791 [93] Sabahudin Hrapovic, Y. L., and John H. T. Luong. (2007). Reusable Platinum Nanoparticle Modified Boron  
792 Doped Diamond Microelectrodes for Oxidative Determination of Arsenite. *Anal. Chem.*, 79, 500-507.  
793 <https://doi:10.1021/ac061528a>
- 794 [94] Dai, X., & Compton, R. G. (2006). Detection of As(III) via oxidation to As(V) using platinum nanoparticle modified  
795 glassy carbon electrodes: arsenic detection without interference from copper. *Analyst*, 131(4), 516-521.  
796 <https://doi:10.1039/b513686e>
- 797 [95] Zhang, T., Jin, H., Fang, Y., Guan, J., Ma, S., Pan, Y., Zhang, M., Zhu, H., Liu, X. & Du, M. (2019). Detection  
798 of trace Cd<sup>2+</sup>, Pb<sup>2+</sup> and Cu<sup>2+</sup> ions via porous activated carbon supported palladium nanoparticles modified  
799 electrodes using SWASV. *Mater. Chem. Phys.*, 225, 433-442. <https://doi:10.1016/j.matchemphys.2019.01.010>
- 800 [96] Veerakumar, P., Veeramani, V., Chen, S.-M., Madhu, R., & Liu, S.-B. (2016). Palladium Nanoparticle  
801 Incorporated Porous Activated Carbon: Electrochemical Detection of Toxic Metal Ions. *ACS Applied Materials &*  
802 *Interfaces*, 8(2), 1319–1326. <https://doi:10.1021/acsami.5b10050>
- 803 [97] Lee, P. M., Chen, Z., Li, L., & Liu, E. (2015). Reduced graphene oxide decorated with tin nanoparticles through  
804 electrodeposition for simultaneous determination of trace heavy metals. *Electrochim. Acta*, 174, 207-214.  
805 <https://doi:10.1016/j.electacta.2015.05.092>
- 806 [98] Toghill, K. E., Xiao, L., Wildgoose, G. G., & Compton, R. G. (2009). Electroanalytical Determination of  
807 Cadmium(II) and Lead(II) Using an Antimony Nanoparticle Modified Boron-Doped Diamond Electrode.  
808 *Electroanalysis*, 21(10), 1113-1118. <https://doi:10.1002/elan.200904547>
- 809 [99] George, J. M., Antony, A., & Mathew, B. (2018). Metal oxide nanoparticles in electrochemical sensing and  
810 biosensing: a review. *Mikrochim Acta*, 185(7), 358. <https://doi:10.1007/s00604-018-2894-3>
- 811 [100] Lee, S., Oh, J., Kim, D., & Piao, Y. (2016). A sensitive electrochemical sensor using an iron oxide/graphene  
812 composite for the simultaneous detection of heavy metal ions. *Talanta*, 160, 528-536.  
813 <https://doi:10.1016/j.talanta.2016.07.03>
- 814 [101] Li, S.-S., Zhou, W.-Y., Jiang, M., Li, L.-N., Sun, Y.-F., Guo, Z., Liu, J.-H. & Huang, X.-J. (2018). Insights into  
815 diverse performance for the electroanalysis of Pb(II) on Fe<sub>2</sub>O<sub>3</sub> nanorods and hollow nanocubes: Toward analysis  
816 of adsorption sites. *Electrochimica Acta*. <https://doi:10.1016/j.electacta.2018.08.069>
- 817 [102] Deshmukh, S., Kandasamy, G., Upadhyay, R. K., Bhattacharya, G., Banerjee, D., Maity, D., Roy, S. S. (2017).  
818 Terephthalic acid capped iron oxide nanoparticles for sensitive electrochemical detection of heavy metal ions in  
819 water. *J. Electroanal. Chem.*, 788, 91-98. <https://doi:10.1016/j.jelechem.2017.01.064>
- 820 [103] Sun, Y., Zhang, W., Yu, H., Hou, C., Li, D., Zhang, Y., & Liu, Y. (2015). Controlled synthesis various shapes  
821 Fe<sub>3</sub>O<sub>4</sub> decorated reduced graphene oxide applied in the electrochemical detection. *Journal of Alloys and*  
822 *Compounds*, 638, 182–187. <https://doi:10.1016/j.jallcom.2015.03.061>
- 823 [104] Yantasee, W., Hongsirikarn, K., Warner, C. L., Choi, D., Sangvanich, T., Toloczko, M. B., Timchalk, C. (2008).  
824 Direct detection of Pb in urine and Cd, Pb, Cu, and Ag in natural waters using electrochemical sensors immobilized  
825 with DMSA functionalized magnetic nanoparticles. *Analyst*, 133(3), 348-355. <https://doi:10.1039/b711199a>
- 826 [105] Miao, P., Tang, Y., & Wang, L. (2017). DNA Modified Fe<sub>3</sub>O<sub>4</sub>@Au Magnetic Nanoparticles as Selective Probes  
827 for Simultaneous Detection of Heavy Metal Ions. *ACS Appl. Mater. Interfaces*, 9(4), 3940-3947.  
828 <https://doi:10.1021/acsami.6b14247>
- 829 [106] Cui, H., Yang, W., Li, X., Zhao, H., & Yuan, Z. (2012). An electrochemical sensor based on a magnetic Fe<sub>3</sub>O<sub>4</sub>  
830 nanoparticles and gold nanoparticles modified electrode for sensitive determination of trace amounts of arsenic(iii).  
831 *Analytical Methods*, 4(12). <https://doi:10.1039/c2ay25913c>

- 832 [107] Xiong, S., Wang, M., Cai, D., Li, Y., Gu, N., & Wu, Z. (2013). Electrochemical Detection of Pb(II) by Glassy  
833 Carbon Electrode Modified with Amine-Functionalized Magnetite Nanoparticles. *Anal. Lett.*, 46(6), 912-922.  
834 <https://doi:10.1080/00032719.2012.747094>
- 835 [108] Song, Q., Li, M., Huang, L., Wu, Q., Zhou, Y., & Wang, Y. (2013). Bifunctional polydopamine@Fe<sub>3</sub>O<sub>4</sub> core-  
836 shell nanoparticles for electrochemical determination of lead(II) and cadmium(II). *Anal. Chim. Acta*, 787, 64-70.  
837 <https://doi:10.1016/j.aca.2013.06.010>
- 838 [109] Sun, Y.-F., Chen, W.-K., Li, W.-J., Jiang, T.-J., Liu, J.-H., & Liu, Z.-G. (2014). Selective detection toward Cd<sup>2+</sup>  
839 using Fe<sub>3</sub>O<sub>4</sub>/RGO nanoparticle modified glassy carbon electrode. *J. Electroanal. Chem.*, 714-715, 97-102.  
840 <https://doi:10.1016/j.jelechem.2013.12.030>
- 841 [110] Fan, H.-L., Zhou, S.-F., Gao, J., & Liu, Y.-Z. (2016). Continuous preparation of Fe<sub>3</sub>O<sub>4</sub> nanoparticles through  
842 Impinging Stream-Rotating Packed Bed reactor and their electrochemistry detection toward heavy metal ions. *J.*  
843 *Alloys Compd.*, 671, 354-359. <https://doi:10.1016/j.jallcom.2016.02.062>
- 844 [111] Zhou, S.-F., Han, X.-J., & Liu, Y.-Q. (2016). SWASV performance toward heavy metal ions based on a high-  
845 activity and simple magnetic chitosan sensing nanomaterials. *J. Alloys Compd.*, 684, 1-7.  
846 <https://doi:10.1016/j.jallcom.2016.05.152>
- 847 [112] Baghayeri, M., Amiri, A., Maleki, B., Alizadeh, Z., & Reiser, O. (2018). A simple approach for simultaneous  
848 detection of cadmium(II) and lead(II) based on glutathione coated magnetic nanoparticles as a highly selective  
849 electrochemical probe. *Sens. Actuators, B* 273, 1442-1450. <https://doi:10.1016/j.snb.2018.07.063>
- 850 [113] Rasha A. Ahmed, A. M. F. (2013). Preparation and Characterization of a Nanoparticles Modified Chitosan  
851 Sensor and Its Application for the Determination of Heavy Metals from Different Aqueous Media. *Int. J. Electrochem.*  
852 *Sci.*, 8, 6692 - 6708.
- 853 [114] Filik, H., & Avan, A. A. (2019). Dextran modified magnetic nanoparticles based solid phase extraction coupled  
854 with linear sweep voltammetry for the speciation of Cr(VI) and Cr(III) in tea, coffee, and mineral water samples.  
855 *Food Chemistry*, 292, 151–159. <https://doi:10.1016/j.foodchem.2019.04.058>
- 856 [115] Yang, H., Liu, X., Fei, R., & Hu, Y. (2013). Sensitive and selective detection of Ag<sup>+</sup> in aqueous solutions using  
857 Fe<sub>3</sub>O<sub>4</sub>@Au nanoparticles as smart electrochemical nanosensors. *Talanta*, 116, 548-553.  
858 <https://doi:10.1016/j.talanta.2013.07.041>
- 859 [116] Dedelaite, L., Kizilkaya, S., Incebay, H., Ciftci, H., Ersoz, M., Yazicigil, Z., Ramanavicius, A. (2015).  
860 Electrochemical determination of Cu(II) ions using glassy carbon electrode modified by some nanomaterials and 3-  
861 nitroaniline. *Colloids Surf., A*, 483, 279-284. <https://doi:10.1016/j.colsurfa.2015.05.054>
- 862 [117] Afkhami, A., Moosavi, R., Madrakian, T., Keypour, H., Ramezani-Aktij, A., & Mirzaei-Monsef, M. (2014).  
863 Construction and Application of an Electrochemical Sensor for Simultaneous Determination of Cd(II), Cu(II) and  
864 Hg(II) in Water and Foodstuff Samples. *Electroanalysis*, 26(4), 786-795. <https://doi:10.1002/elan.201300619>
- 865 [118] Zhou, S.-F., Han, X.-J., Fan, H.-L., Zhang, Q.-X., & Liu, Y.-Q. (2015). Electrochemical detection of As(III)  
866 through mesoporous MnFe<sub>2</sub>O<sub>4</sub> nanocrystal clusters by square wave stripping voltammetry. *Electrochim. Acta*, 174,  
867 1160-1166. <https://doi:10.1016/j.electacta.2015.06.036>
- 868 [119] Zhou, S., Han, X., Fan, H., & Liu, Y. (2016). Electrochemical Sensing toward Trace As(III) Based on  
869 Mesoporous MnFe<sub>2</sub>O<sub>4</sub>/Au Hybrid Nanospheres Modified Glass Carbon Electrode. *Sensors (Basel)*, 16(6).  
870 <https://doi:10.3390/s16060935>
- 871 [120] Han, X.-J., Zhou, S.-F., Fan, H.-L., Zhang, Q.-X., & Liu, Y.-Q. (2015). Mesoporous MnFe<sub>2</sub>O<sub>4</sub> nanocrystal  
872 clusters for electrochemistry detection of lead by stripping voltammetry. *Journal of Electroanalytical Chemistry*, 755,  
873 203–209. <https://doi:10.1016/j.jelechem.2015.07.054>
- 874 [121] Zhou, S.-F., Han, X.-J., Fan, H.-L., Huang, J., & Liu, Y.-Q. (2018). Enhanced electrochemical performance for  
875 sensing Pb(II) based on graphene oxide incorporated mesoporous MnFe<sub>2</sub>O<sub>4</sub> nanocomposites. *J. Alloys Compd.*,  
876 747, 447-454. <https://doi:10.1016/j.jallcom.2018.03.037>
- 877 [122] Zhou, S.-F., Wang, J.-J., Gan, L., Han, X.-J., Fan, H.-L., Mei, L.-Y., Liu, Y.-Q. (2017). Individual and  
878 simultaneous electrochemical detection toward heavy metal ions based on L-cysteine modified mesoporous  
879 MnFe<sub>2</sub>O<sub>4</sub> nanocrystal clusters. *J. Alloys Compd.*, 721, 492-500. <https://doi:10.1016/j.jallcom.2017.05.321>
- 880 [123] Salimi, A., Mamkhezri, H., Hallaj, R., & Soltanian, S. (2008). Electrochemical detection of trace amount of  
881 arsenic(III) at glassy carbon electrode modified with cobalt oxide nanoparticles. *Sens. Actuators, B*, 129(1), 246-  
882 254. <https://doi:10.1016/j.snb.2007.08.017>
- 883 [124] Zhou, L., Xiong, W., & Liu, S. (2014). Preparation of a gold electrode modified with Au–TiO<sub>2</sub> nanoparticles as  
884 an electrochemical sensor for the detection of mercury(II) ions. *J. Mater. Sci.* 50(2), 769-776.  
885 <https://doi:10.1007/s10853-014-8636-y>

- 886 [125] Zhang, X., Zeng, T., Hu, C., Hu, S., & QiulinTian, Q. (2016). Studies on fabrication and application of arsenic  
887 electrochemical sensors based on titanium dioxide nanoparticle modified gold strip electrodes. *Analytical Methods*,  
888 8(5), 1162-1169. <https://doi:10.1039/c5ay02397a>
- 889 [126] Mao, A., Li, H., Cai, Z., & Hu, X. (2015). Determination of mercury using a glassy carbon electrode modified  
890 with nano TiO<sub>2</sub> and multi-walled carbon nanotubes composites dispersed in a novel cationic surfactant. *Journal of*  
891 *Electroanalytical Chemistry*, 751, 23–29. <https://doi:10.1016/j.jelechem.2015.04.034>
- 892 [127] Ramezani, S., Ghobadi, M., & Bideh, B. N. (2014). Voltammetric monitoring of Cd (II) by nano-TiO<sub>2</sub> modified  
893 carbon paste electrode sensitized using 1,2-bis-[o-aminophenyl thio] ethane as a new ion receptor. *Sensors and*  
894 *Actuators B: Chemical*, 192, 648–657. <https://doi:10.1016/j.snb.2013.11.033>
- 895 [128] Liu, F., Zhang, Y., Yin, W., Hou, C., Huo, D., He, B., Qian, L. & Fa, H. (2017). A high-selectivity electrochemical  
896 sensor for ultra-trace lead (II) detection based on a nanocomposite consisting of nitrogen-doped graphene/gold  
897 nanoparticles functionalized with ETBD and Fe<sub>3</sub>O<sub>4</sub>@TiO<sub>2</sub> core-shell nanoparticles. *Sensors and Actuators B:*  
898 *Chemical*, 242, 889–896. <https://doi:10.1016/j.snb.2016.09.167>
- 899 [129] Zhang, Q.-X., Wen, H., Peng, D., Fu, Q., & Huang, X.-J. (2015). Interesting interference evidences of  
900 electrochemical detection of Zn(II), Cd(II) and Pb(II) on three different morphologies of MnO<sub>2</sub> nanocrystals. *J.*  
901 *Electroanal. Chem.*, 739, 89-96. <https://doi:10.1016/j.jelechem.2014.12.023>
- 902 [130] Fayazi, M., Taher, M. A., Afzali, D., & Mostafavi, A. (2016). Fe<sub>3</sub>O<sub>4</sub> and MnO<sub>2</sub> assembled on halloysite  
903 nanotubes: A highly efficient solid-phase extractant for electrochemical detection of mercury(II) ions. *Sensors and*  
904 *Actuators B: Chemical*, 228, 1–9. <https://doi:10.1016/j.snb.2015.12.107>
- 905 [131] Salimi, A., Pourbahram, B., Mansouri-Majd, S., & Hallaj, R. (2015). Manganese oxide nanoflakes/multi-walled  
906 carbon nanotubes/chitosan nanocomposite modified glassy carbon electrode as a novel electrochemical sensor for  
907 chromium (III) detection. *Electrochimica Acta*, 156, 207–215. <https://doi:10.1016/j.electacta.2014.12.146>
- 908 [132] Wei, Y., Gao, C., Meng, F.-L., Li, H.-H., Wang, L., Liu, J.-H., & Huang, X.-J. (2011). SnO<sub>2</sub>/Reduced Graphene  
909 Oxide Nanocomposite for the Simultaneous Electrochemical Detection of Cadmium(II), Lead(II), Copper(II), and  
910 Mercury(II): An Interesting Favorable Mutual Interference. *The Journal of Physical Chemistry C*, 116(1), 1034–1041.  
911 <https://doi:10.1021/jp209805c>
- 912 [133] Yang, M., Jiang, T.-J., Guo, Z., Liu, J.-H., Sun, Y.-F., Chen, X., & Huang, X.-J. (2017). Sensitivity and  
913 selectivity sensing cadmium(II) using amination functionalized porous SnO<sub>2</sub> nanowire bundles-room temperature  
914 ionic liquid nanocomposite: Combined efficient cation capture with control experimental conditions. *Sensors and*  
915 *Actuators B: Chemical*, 240, 887–894. <https://doi:10.1016/j.snb.2016.09.060>
- 916 [134] Cui, X., Fang, X., Zhao, H., Li, Z., & Ren, H. (2018). Fabrication of thiazole derivatives functionalized graphene  
917 decorated with fluorine, chlorine and iodine@SnO<sub>2</sub> nanoparticles for highly sensitive detection of heavy metal ions.  
918 *Colloids and Surfaces A: Physicochemical and Engineering Aspects*, 546, 153–162.  
919 <https://doi:10.1016/j.colsurfa.2018.03.004>
- 920 [135] Li, Y., Liu, X. R., Ning, X. H., Huang, C. C., Zheng, J. B., & Zhang, J. C. (2011). An ionic liquid supported  
921 CeO<sub>2</sub> nanoparticles-carbon nanotubes composite-enhanced electrochemical DNA-based sensor for the detection  
922 of Pb(2). *J. Pharm. Anal.*, 1(4), 258-263. <https://doi:10.1016/j.jpha.2011.09.001>
- 923 [136] Yukird, J., Kongsittikul, P., Qin, J., Chailapakul, O., Rodthongkum, N. (2018) ZnO@graphene nanocomposite  
924 modified electrode for sensitive and simultaneous detection of Cd (II) and Pb (II). *Synth. Met.* 245, 251–259.  
925 <https://doi.org/10.1016/j.synthmet.2018.09.012>
- 926 [137] Yuan-Yuan, L., Meng-Ni, C., Yi-Li, G., Jian-Mao, Y., Xiao-Yu, M.A., Jian-Yun, L. (2015) Preparation of zinc  
927 oxide-graphene composite modified electrodes for detection of trace Pb(II). *Chinese J. Anal. Chem.* 43, 1395–1401.  
928 [https://doi.org/10.1016/s1872-2040\(15\)60862-3](https://doi.org/10.1016/s1872-2040(15)60862-3)
- 929 [138] Wei, Y., Yang, R., Yu, X.-Y., Wang, L., Liu, J.-H., & Huang, X.-J. (2012). Stripping voltammetry study of ultra-  
930 trace toxic metal ions on highly selectively adsorptive porous magnesium oxide nanoflowers. *The Analyst*, 137(9),  
931 2183. <https://doi:10.1039/c2an15939b>
- 932
- 933